

Reactions of a Cyclodimethylsiloxane (Me₂SiO)₆ with Silver Salts of Weakly Coordinating Anions; Crystal Structures of [Ag(Me₂SiO)₆][Al] ([Al] = [Al(OR_F)₄], [Al(OR_F)₃]) and Their Comparison with [Ag(18-Crown-6)]₂[SbF₆]₂

T. Stanley Cameron,[†] Andreas Decken,[‡] Ingo Krossing,[§] Jack Passmore,^{*,‡} J. Mikko Rautiainen,^{*,||} Xinpeng Wang,[⊥] and Xiaoqing Zeng[⊗]

[†]Department of Chemistry, Dalhousie University, Halifax, Nova Scotia, B3H 4J3, Canada

[‡]Department of Chemistry, University of New Brunswick, Fredericton, New Brunswick, E3B 5A3, Canada

[§]Institute for Inorganic and Analytical Chemistry, Albert–Ludwigs–Universität Freiburg, Albertstrasse 21, 79104 Freiburg, Germany

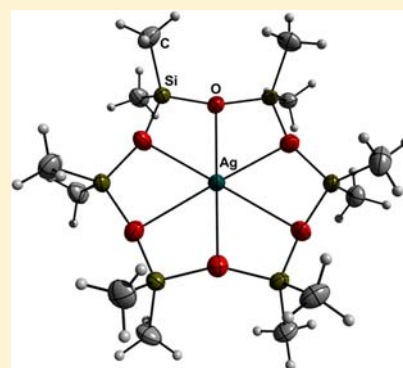
^{||}Department of Chemistry, University of Oulu, P.O. Box 3000, Oulu, 90014, Finland

[⊥]State Key Laboratory of Coordination Chemistry, Nanjing University, Nanjing 210093, P.R.China

[⊗]Division C–Inorganic Chemistry, University of Wuppertal, Gaußstrasse 20, 42119 Wuppertal, Germany

Supporting Information

ABSTRACT: Two silver-cyclodimethylsiloxane cation salts [AgD₆][Al] ([Al] = [Al(OR_F)₄]⁻ (1) or [Al(OR_F)₃]⁻ (2), R_F = C(CF₃)₃, D = Me₂SiO) were prepared by the reactions of Ag[Al] with D₆ in SO₂(l). For a comparison the [Ag(18-crown-6)]₂[SbF₆]₂ (3) salt was prepared by the reaction of Ag[SbF₆] and 18-crown-6 in SO₂(l). The compounds were characterized by IR, multinuclear NMR, and single crystal X-ray crystallography. The structures of 1 and 2 show that D₆ acts as a pseudo crown ether toward Ag⁺. The stabilities and bonding of [MD_n]⁺ and [M(18-crown-6)]⁺ (M = Ag, Li, n = 4–8) complexes were studied with theoretical calculations. The calculations predicted that D₆ adopts a puckered C₃ symmetric structure in the gas phase in contrast to previous reports. 18-Crown-6 was calculated to bind more strongly to Li⁺ and Ag⁺ than D₆. ²⁹Si[¹H] NMR results in solution, and calculations in the gas phase established that a hard Lewis acid Li⁺ binds more strongly to D₆ than Ag⁺. A comparison of the [MD_n]⁺ complex stabilities showed D₇ to form the most stable metal complexes in the gas phase and the solid state and explained why [AgD₇][SbF₆] was isolated in a previous reaction where ring transformations resulted in an equilibrium of [AgD_n]⁺ complexes. In contrast, the isolations of 1 and 2 were possible because the corresponding equilibrium of [AgD_n]⁺ complexes was not observed with [Al]⁻ anions. The formation of the dinuclear complex salt 3 instead of the corresponding mononuclear complex salt was shown to be driven by the gain in lattice enthalpy in the solid state. The bonding to Li⁺ in D₆ and 18-crown-6 metal complexes was described by a quantum theory of atoms in molecules (QTAIM) analysis to be mostly electrostatic while the bonding to Ag⁺ also had a significant charge transfer component. The charge transfer from both D₆ and 18-crown-6 to Ag⁺ and Li⁺ metal ions was depicted by the QTAIM analysis to be of similar strength, and the difference in the stabilities of the complexes was attributed mostly to more attractive electrostatic interactions between 18-crown-6 and the metal ions despite the more negative oxygen atomic charges calculated for D₆.



1. INTRODUCTION

The importance of crown ethers¹ as metal complexing agents and their role in the development of host guest chemistry is undeniable,² culminating in Pedersen's 1987 Nobel Prize in Chemistry³ shared with Lehn and Cram. In contrast to the wide variety of crown ether metal complexes, the metal complexes of analogous silicon-containing macrocyclic ethers, dimethylsiloxanes D_n (D_n = (Me₂SiO)_n, n = 3 – 40) are rare⁴ despite the widespread use of cyclic dimethylsiloxanes in industrial applications and consumer products.⁵ The first examples of D_n metal complexes, two potassium complexes of D₇ K₃[KD₇][InNp₃H]₄ (Np = neopentyl)⁶ and [KD₇][C(SiMe₃)₂{SiMe₂(CH=CH₂)}]₇

were reported in the 1990s as results of serendipitous reactions between highly reactive species and silicon grease. More recently the presence of silicon grease in a reaction mixture designed to give Se₆Ph₂[Al(OR_F)₄] (R_F = C(CF₃)₃) resulted in the isolation of crystals of [LiD₆][Al(OR_F)₄] and subsequently the synthesis of [LiD_n][Al(OR_F)₄] (n = 5,6; R_F = C(CF₃)₃, C(CF₃)₂Ph) via direct reactions between lithium salts and dimethylsiloxanes.⁸ Silicon grease has also been reported to take part in the bromination reaction of Zr(C₃H₅)₂Br₂ giving [ZrD₇Br₂][Zr₂Br₉]₂ as a

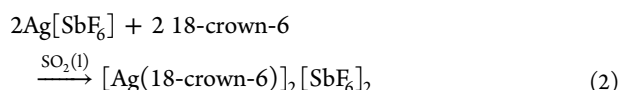
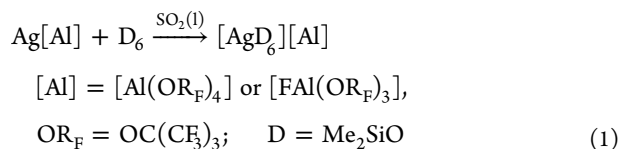
Received: November 26, 2012

Published: February 27, 2013

byproduct.⁹ The reactions of D_n ($n = 3-6$) with $\text{Ag}[\text{SbF}_6]$ in $\text{SO}_2(\text{l})$ gave rise to ring transformation reactions.¹⁰ The ring transformation reactions have been suggested to be cation induced and to proceed through a fluoride abstraction from $[\text{SbF}_6]^-$ and an intermediate $\text{FSiMe}_2(\text{OSiMe})_{m-2}\text{OSiMeO}^-$ anion resulting in a mixture of the most thermodynamically favored $[\text{AgD}_n]^+$ ($n = 6-8$) species (GC-MS, $^{29}\text{Si}\{^1\text{H}\}$ NMR) and the isolation of $[\text{AgD}_7][\text{SbF}_6]$ (XRD). The parent Lewis acids of large weakly coordinating anions $[\text{Al}]^-$ $\{[\text{Al}] = [\text{Al}(\text{OR}_F)_4]$ or $[\text{FAl}(\text{OR}_F)_3]$, $\text{R}_F = \text{C}(\text{CF}_3)_3\}$ have higher fluoride ion affinities than SbF_5 (cf. calc. SbF_5 489 vs $[\text{Al}\{\text{OC}(\text{CF}_3)_3\}_3]$ 537 kJ mol^{-1})¹¹ and therefore the $[\text{Al}]^-$ salts are less likely to take part in the D_n ring transformation reactions. A lithium induced ring-opening polymerization mechanism has also been suggested for the reaction between D_3 and *tert*-butyllithium that gives linear polydimethylsiloxanes.¹²

In this contribution we describe the preparation of two silver-cyclodimethylsiloxane cation salts $[\text{AgD}_6][\text{Al}(\text{OR}_F)_4]$ (**1**) and $[\text{AgD}_6][\text{FAl}(\text{OR}_F)_3]$ (**2**). **2** was first found as crystals in a complex reaction mixture, and its structure showed ion pairs.¹³ In the hope of getting a more ionic structure **1** was prepared by a direct reaction between D_6 and the more readily available $\text{Ag}[\text{Al}(\text{OR}_F)_4]$ (eq 1), and later **2** was also obtained via a direct reaction. The direct preparation of **1** and **2** from their components supports the suggested route for D_n ring transformation reactions.¹⁰ The stabilities and bonding of **1** and **2** have been compared with the silver(I) complex of analogous crown ether 18-crown-6.

No silver 18-crown-6 complex structures had been reported prior to 2002.¹⁴ Since then some silver 18-crown-6 complex salts have been characterized, for example, $[\text{Ag}(18\text{-crown-6})(\text{H}_2\text{O})(\text{NO}_3)]$,¹⁵ $[\text{Ag}(18\text{-crown-6})(\text{CF}_3\text{SO}_3)]$,¹⁵ and $[\text{Ag}_4(18\text{-crown-6})_4(\text{H}_2\text{O})_3][\text{Ag}_{18}(\text{C}_2)_3(\text{CF}_3\text{CO}_2)_{16}(\text{H}_2\text{O})_{2,5}]\cdot 2.5\text{H}_2\text{O}$.¹⁶ In these reported crystal structures significant coordination from solvent molecules or counteranions to the silver 18-crown-6 complexes is present. As a part of our effort to compare the bonding between the cyclic dimethylsiloxane metal complexes and the cyclic ether metal complexes we synthesized a solvent free $[\text{SbF}_6]^-$ salt of the $[\text{Ag}(18\text{-crown-6})]^+$ complex to minimize the effect anions and solvent molecules have on the complex structure. However instead of the expected simple $[\text{Ag}(18\text{-crown-6})][\text{SbF}_6]$ complex salt we obtained a dinuclear $[\text{Ag}(18\text{-crown-6})]_2[\text{SbF}_6]_2$ (**3**) complex (eq 2). The synthesis and characterization of **3** is described.



The differences in the observed stabilities of siloxane and ether complexes have been associated with low basicity of oxygen in siloxanes.¹⁷ The low basicity of siloxanes has been previously explained as due to $p^2(\text{O}) \rightarrow \sigma^*(\text{Si-R})$ negative hyperconjugation¹⁸ or the spatially diffuse oxygen electron pairs that result from the high electronegativity difference between oxygen and silicon and thus the high ionic nature of O–Si bonds.^{19,20} Our theoretical studies on Li^+ and Ag^+ metal complexes of $\text{O}(\text{SiH}_2\text{Me})_2$ and OEt_2 have shown the $\text{O}(\text{SiH}_2\text{Me})_2$ complexes to be less stable than the OEt_2 complexes despite

the more negative oxygen atomic charges on $\text{O}(\text{SiH}_2\text{Me})_2$ that would suggest stronger electrostatic attraction with the metal cations.²¹ The repulsion between the positively charged silicon atoms and the metal ions was shown to counteract the stronger attraction between the oxygen atoms and the metal ions in the $\text{O}(\text{SiH}_2\text{Me})_2$ complexes. Furthermore, the presence of metal cations was shown to cause changes in the bonding and polarization of the ligands in a way that resulted in the lower stability of the $\text{O}(\text{SiH}_2\text{Me})_2$ complexes, that is, the further polarization of the already polar O–Si bonds in 1,3-dimethyldisiloxane caused the energy of 1,3-dimethyldisiloxane to rise more than the polarization of O–C bonds raised the energy of diethyl ether.

2. EXPERIMENTAL SECTION

2.1. General Experimental Technique. All manipulations were performed by using standard closed vacuum line techniques, grease free metal apparatus, and drybox techniques under nitrogen atmosphere.²² The compounds $\text{Ag}[\text{Al}(\text{OR}_F)_4]$ ^{23a} and $\text{Ag}[\text{FAl}(\text{OR}_F)_3]$ ($\text{R}_F = \text{C}(\text{CF}_3)_3$)^{23b} were prepared as described in the literature. D_6 (Gelest, $\geq 95\%$) ($D = \text{Me}_2\text{SiO}$) was used as delivered. 18-Crown-6 (Fluka, $\geq 99\%$) was recrystallized from acetonitrile and vacuum-dried. $\text{Ag}[\text{SbF}_6]$ (SynQuest, $\geq 99\%$) was purified by dissolving in liquid SO_2 and filtering through a medium frit in the absence of light, so that the reagent was snow-white. Sulfur dioxide (Matheson, anhydrous, 99.85%) was dried and stored over CaH_2 and freshly distilled before use. Diethyl ether was obtained from a solvent purification system and stored over sodium metal before use. NMR spectra were recorded on a Varian 400 NMR spectrometer. ^1H , ^{13}C , and $^{29}\text{Si}\{^1\text{H}\}$ chemical shifts were reported in δ units downfield from Me_4Si in SO_2 as the reference signal. CFCl_3 (in D_2O) and AlCl_3 (in D_2O) were used as references for measuring ^{19}F and ^{27}Al spectra, respectively. NMR samples were prepared in 10 mm thick walled NMR tubes fitted with J. Young valves using SO_2 as solvent. FT-IR spectra were recorded using a Thermo Nicolet spectrometer (Nexus 470 FT-IR).

2.2. Crystal Structures. Single crystals were coated with Paratone-N oil, mounted using a polyimide MicroMount and frozen in the cold nitrogen stream of the goniometer. Crystal data were recorded on a Rigaku RAXIS (**1**) and a Bruker AXS P4/SMART 1000 (**2** and **3**) diffractometers. Crystalstructure 3.8²⁴ (**1**) and SHELX version 6.1²⁵ program packages (**2** and **3**) were used for the structure solutions and the refinements. The crystal structures were solved by direct methods and refined by full-matrix least-squares procedures. All non-hydrogen atoms were refined anisotropically. Hydrogen atoms were included at calculated positions and refined using a riding model. A summary of the data collection parameters is provided in Table 1. All figures illustrating crystal structures have been prepared using DIAMOND program.²⁶

2.3. Computational Details. All density functional theory (DFT) calculations were carried out with the Gaussian 09 program package.²⁷ The M06-L local functional²⁸ and 6-311++G(2d,p) basis set²⁹ (and aug-cc-pVTZ-PP for silver)³⁰ with ultrafine integration grids were employed in the DFT calculations. Quantum theory of atoms in molecules (QTAIM) analyses were carried out with AIMAll program.³¹ The optimized structures have been drawn using ChemCraft program.³²

2.4. Syntheses. Synthesis of 1. All reactions in SO_2 were carried out in a jointless Pyrex apparatus consisting of two tubes (OD 3 cm) equipped with two Teflon in glass Rotaflo (6 HK) valves and joined by a glass tube that incorporated a medium sintered frit as previously described in reference 22. D_6 (0.23 mL, 0.49 mmol) was added onto $\text{Ag}[\text{Al}(\text{OR}_F)_4]$ (0.532 g, 0.51 mmol) that was in one tube of a two-tube vessel. The vessel was cooled with liquid N_2 and degassed. SO_2 (7 mL) was condensed onto the mixture and warmed to room temperature. This mixture was stirred overnight at room temperature and then filtered. Colorless crystals were obtained by evaporating the volatiles from the resulting clear solution at 5 °C. The crystals were washed three times with SO_2 and the volatiles were removed under vacuum. Yield: 0.652 g (89% yield based on D_6). mp 177 °C (decomp).

Table 1. Selected X-ray Crystallographic Data for 1, 2, and 3

	1	2	3
formula	C ₂₈ H ₃₆ AgAlF ₃₆ O ₁₀ Si ₆	C ₂₄ H ₃₆ AgAlF ₂₈ O ₉ Si ₆	C ₁₂ H ₂₄ AgF ₆ O ₆ Sb
formula wt	1519.89	1303.92	607.93
T [K]	98(1)	173(1)	173(1)
space group	P $\bar{1}$	P2(1)/n	P $\bar{1}$
crystal system	triclinic	monoclinic	triclinic
color and habit	colorless, block	colorless, plate	colorless, irregular
a [Å]	14.2609(5)	12.990(3)	9.1671(15)
b [Å]	21.3122(9)	21.368(4)	9.6508(16)
c [Å]	21.6672(11)	18.082(4)	11.996(2)
α [deg]	115.3870(12)		105.639(2)
β [deg]	98.150(1)	93.199(4)	91.602(2)
γ [deg]	103.4840(7)		106.652(2)
V [Å ³]	5562.1(4)	5011.3(18)	972.7(3)
Z	4	4	2
density [g cm ⁻³]	1.815	1.728	2.076
μ , mm ⁻¹	0.673	0.709	2.475
collected reflections	25020	34368	6753
independent reflections	13123	11207	4222
R1, wR2	0.0681, 0.0797	0.0686, 0.2163	0.0243, 0.0648

¹³C{¹H} NMR (100.6 MHz, SO₂, RT): δ = 120.6 ppm (q, J(C–F) = 291 Hz, 3C, CF₃), 79.9 ppm (s, 1C, C(CF₃)₃), 0.1 ppm (q, 3C, SiMe₂); ²⁹Si{¹H} NMR (79.4 MHz, SO₂, RT): δ = –11.1 ppm (s, AgD₆⁺); ¹⁹F NMR (376.3 MHz, SO₂, RT): δ = –75.3 ppm (s, CF₃); ²⁷Al NMR (104.2 MHz, SO₂, RT): δ = 34.9 ppm (s, [Al(OR_F)₄]); ¹H NMR (399.9 MHz, SO₂, RT): δ = 1.11 ppm (s, SiMe₂). IR (KBr, Neat, RT, ν assigned to [AgD₆]⁺ marked with *): $\nu_{\max}/\text{cm}^{-1}$ = 2964 (w),* 2913 (vw),* 1457 (vw),* 1416 (vw),* 1400 (w),* 1352 (m),* 1302 (m),* 1275 (s),* 1242 (m),* 1220 (vs),* 1166 (m),* 1135 (w),* 1090 (m); $\nu_{\text{as}}(\text{SiOSi})$,* 1018 (s),* 974 (s),* 855 (m),* 820 (m),* 803 (m); $\nu_{\text{as}}(\text{SiC}_2)$,* 755 (w); $\nu_{\text{as}}(\text{SiC}_2)$,* 728 (m),* 708 (m); $\nu_{\text{s}}(\text{SiC}_2)$,* 657 (w); $\nu_{\text{s}}(\text{SiOSi})$,* 613 (vw), $\nu_{\text{s}}(\text{SiOSi})$,* 571 (vw),* 560 (w),* 536 (w),* 509 (m),* 445 (m),* 383 (m),* 353 (m)* (see the Supporting Information, Figure S1.1 for the IR spectrum and Supporting Information, Table S1.1 for the assignments).

Synthesis of 2. The preparation is similar to that of 1. (Ag[FAl(OR_F)₃]) 1.096 g, 1.28 mmol; D₆ 0.5 mL, 1.08 mmol; SO₂ 12 mL. Yield: 0.581 g (41% yield based on D₆). mp 124 °C (decomp). ¹³C{¹H} NMR (100.6 MHz, SO₂, RT): δ = 120.7 ppm (q, 3C, J(C–F) = 291 Hz, CF₃), 79.7 ppm (s, 1C, C(CF₃)₃), 0.5 ppm (q, 3C, SiMe₂); ²⁹Si{¹H} NMR (79.4 MHz, SO₂, RT): δ = –14.2 ppm (s, AgD₆⁺); ¹⁹F NMR (376.3 MHz, SO₂, RT): δ = –75.1 ppm (s, CF₃), –176.3 ppm (s, FAl(OR_F)₃); ²⁷Al NMR (104.2 MHz, SO₂, RT): δ = 40.8 ppm (d, J(Al–F) = 68 Hz, [FAl(OR_F)₃]); ¹H NMR (399.9 MHz, SO₂, RT): δ = 1.34 ppm (s, SiMe₂). IR (KBr, Neat, RT, ν assigned to [AgD₆]⁺ marked with *): $\nu_{\max}/\text{cm}^{-1}$ = 2964 (m),* 2906 (w),* 1456 (vw),* 1414 (w),* 1400 (w),* 1351 (w),* 1300 (m),* 1272 (vs),* 1240 (m),* 1221 (s),* 1192 (m),* 1167 (m),* 1068 (vs); $\nu_{\text{as}}(\text{SiOSi})$,* 1012 (vs),* 974 (vs),* 854 (m),* 817 (m),* 803 (s); $\nu_{\text{as}}(\text{SiC}_2)$,* 755 (m); $\nu_{\text{as}}(\text{SiC}_2)$,* 727 (s),* 709 (m); $\nu_{\text{s}}(\text{SiC}_2)$,* 672 (w); $\nu_{\text{s}}(\text{SiOSi})$,* 658 (w); $\nu_{\text{s}}(\text{SiOSi})$,* 612 (w); $\nu_{\text{s}}(\text{SiOSi})$,* 564 (m),* 536 (m),* 449 (m),* 389 (m),* 354 (w) (see the Supporting Information, Figure S1.2 for the IR spectrum and Supporting Information, Table S1.1 for the assignments).

Synthesis of 3. A vessel similar to that in 1 was used for the reaction. Ag[SbF₆] (1.207 g, 3.51 mmol) and 18-crown-6 (0.742 g, 2.81 mmol) were added to separate tubes of the reaction vessel. The vessel was degassed, and SO₂ (4 mL) was condensed into the vessel to dissolve both solids. The solution of 18-crown-6 was poured onto the solution of Ag[SbF₆]. Some gray precipitate was formed upon mixing the solutions. The resulting solution was filtered, and the volatiles were removed yielding 1.692 g (2.78 mmol; 99% yield based on 18-crown-6 and eq 2) of the white crude product. Using a similar reaction vessel as above a small amount of crude product (0.110 g) was dissolved in SO₂ (3 mL). A small amount of diethyl ether was condensed into the solution resulting in the precipitation of the least soluble portion of the crude product. This solution was filtered, and more diethyl ether

(10 mL) was condensed onto the solution. Colorless crystals (collected amount 0.080 g) were obtained by slow removal of volatiles at 5 °C by condensation using an ice–water bath. Mp 196 °C (decomp). ¹³C NMR (100.6 MHz, SO₂, RT): δ = 69.4 ppm (t, J(C–H) = 144 Hz, CH₂); ¹⁹F NMR (376.3 MHz, SO₂, RT): δ = –115.2 ppm (sextet, J(F–¹²¹Sb) = 1946 (±14) Hz; octet, J(F–¹²³Sb) = 1054 (±21) Hz, [SbF₆]); ¹H NMR (399.9 MHz, SO₂, RT): δ = 4.73 ppm (d, J²(H–H) = 10 Hz, CH₂). IR (KBr, Neat, RT, ν assigned to [Ag(18-crown-6)]⁺ marked with *): $\nu_{\max}/\text{cm}^{-1}$ = 2909 (m),* 2871 (m),* 1489 (vw),* 1474 (w),* 1461 (w),* 1451 (w),* 1436 (vw),* 1419 (vw),* 1394 (vw),* 1387 (vw),* 1374 (vw),* 1353 (m),* 1300 (m),* 1291 (w),* 1249 (m),* 1237 (w),* 1140 (w),* 1106 (vs),* 1077 (m),* 1065 (m),* 1053 (m),* 1035 (m),* 963 (m),* 955 (m),* 937 (m),* 915 (w),* 866 (m),* 834 (m),* 654 (vs),* 575 (m),* 566 (w),* 520 (m),* 403 (vw)* (See Supporting Information, Figure S1.3 for the IR spectrum and Supporting Information, Table S1.2 for the assignments).

3. RESULTS AND DISCUSSION

3.1. Syntheses and Spectroscopic Characterizations.

The reactions of Ag[Al] ([Al] = [FAl(OR_F)₃], [Al(OR_F)₄]) with liquid D₆ (1: 1) in liquid SO₂ according to eq 1 led to colorless, thermally stable salts. Crystalline material was afforded by cooling of their saturated SO₂ solutions. Single crystal X-ray diffraction gave structures formulated as 1 and 2. Their IR spectra show the characteristic peaks of the anion, and the remaining peaks were very similar to the reactant siloxane D₆ (see the Supporting Information, Figures S1.1 and S1.2).

The ¹⁹F NMR spectra of 1 and 2 in liquid SO₂ have one sharp peak (Table 2: 1 –75.3 ppm; 2 –75.1 ppm), which is

Table 2. ¹⁹F and ²⁹Si{¹H} Chemical Shifts of 1, 2, and Some Reference Compounds in SO₂(l)

compound	¹⁹ F	²⁹ Si{ ¹ H}
D ₆ ^a		–22.7
1	–75.3	–11.1
2	–75.1, –176.3	–14.2
[AgD ₆][SbF ₆] (in situ) ^a		–14.2
[LiD ₆][Al(OR _F) ₄] ^b	–75.3	–9.2
[LiD ₆][Al(OR _{PhF}) ₄] ^b	–74.1	–10.1

^aRef 10. ^bRef 8. R_F = C(CF₃)₃, R_{PhF} = C(Ph)(CF₃)₂.

assigned to –CF₃ fluorine.^{23a} The ¹⁹F NMR spectrum of 2 gives an additional peak (–176.3 ppm) corresponding to –AlF fluorine.^{23b} The ²⁹Si{¹H} NMR spectra of 1 and 2 in SO₂(l) have one peak indicative of one silicon species in solution (Table 2). The ²⁹Si{¹H} chemical shift of 2 (–14.2 ppm) is similar to that of [AgD₆][SbF₆] (–14.2 ppm)¹⁰ but about 3.1 ppm different from that of 1 (–11.1 ppm), depicting a stronger coordination between D₆ and Ag⁺ in 1. This suggests a stronger coordination from [SbF₆][–] and [FAl(OR_F)₃][–] anions to [AgD₆]⁺ ions in SO₂(l) solutions of [AgD₆][SbF₆] and 2 compared to 1 that is more dissociated into [AgD₆]⁺ and [Al{OC(CF₃)₃}₄][–] ions. With the same anion [Al{OC(CF₃)₃}₄][–], the ²⁹Si{¹H} NMR of 1 is at about 1.9 ppm lower field than that of [LiD₆]⁺ (–9.2 ppm), implying a stronger coordination between a hard base (D₆) and a hard acid (Li⁺) in solution than that of Ag⁺. This observation is reflected by the calculated gas phase energetics (see Table 4). The spectroscopic results are consistent with the formation of only one silver-cyclodimethylsiloxane complex [AgD₆]⁺ in contrast to the analogous reaction of Ag[SbF₆] with D₅ that gave a mixture of products.¹⁰

The reaction of Ag[SbF₆] with 18-crown-6 (1:1) in liquid SO₂ according to eq 2 leads to a white, thermally stable salt.

Crystals of the salt (**3**) for single crystal X-ray diffraction were afforded by slow condensation of the solvent from SO₂/diethyl ether mixture. The IR spectrum of **3** (see Supporting Information, Figure S1.3 and Table S1.2) show two bands at 654 and 575 cm⁻¹ characteristic of the [SbF₆]⁻ anion (compare for the 655 and 588 cm⁻¹ bands of the [SbF₆]⁻ anion in (N₅)[SbF₆]³³ and the single 669 cm⁻¹ band of the O_h symmetric [SbF₆]⁻ anion in Li[SbF₆]).³⁴ The IR spectrum indicates a lower symmetry than the ideal O_h symmetry of the [SbF₆]⁻ anions as a result of coordination to the silver atom of the [Ag(18-crown-6)]₂²⁺ complex (see Figure 4d).³⁵ The other bands in the spectrum can be assigned to the [Ag(18-crown-6)]₂²⁺ complex. Free 18-crown-6 is known to crystallize in conformations having D_{3d} and C_i symmetries.³⁶ A comparison of the IR spectrum of **3** with that of a free 18-crown-6 (see Supporting Information, Figure S1.3 and Table S1.2) shows disappearance of bands related to the C_i symmetric conformation (e.g., 993, 1219, and 1444 cm⁻¹) and strengthening of bands related to the D_{3d} symmetric conformation (e.g., 963, 834, and 520 cm⁻¹) indicating that 18-crown-6 has a structure approximating that of a D_{3d} symmetric conformation in the complex. However the IR spectrum of **3** remains more complex than expected for a D_{3d} symmetric complex consistent with the observed crystal structure.

The ¹⁹F NMR spectrum of **3** in liquid SO₂ shows the resonance of [SbF₆]⁻ centered at -115.2 ppm (c.f. Ag[SbF₆]¹⁹F -123 ppm in CH₃CN³⁷ and [TiF₂(18-crown-6)][SbF₆]¹⁹F -114.5 ppm in SO₂)³⁸ with a fine structure due to ¹²¹Sb-¹⁹F and ¹²¹Sb-¹⁹F coupling. The well resolved fine structure indicates that the cations and anions exist as separate species in solution.³⁹ The ¹³C NMR spectrum in SO₂ showed a triplet at 69.5 ppm assigned to CH₂ of [Ag(18-crown-6)]⁺ lying 0.6 ppm upfield from that of a free 18-crown-6, while in the ¹H NMR spectrum of the complex there is a 0.2 ppm downfield shift to 4.73 ppm from that of a free 18-crown-6. A similar small deshielding of ¹³C shifts has been previously observed upon formation of alkali metal 18-crown-6 complexes.⁴⁰ The NMR spectra are consistent with the formation of a silver crown complex in SO₂ solution. However because of rapid exchange in solution, the NMR spectra do not show whether the complex in SO₂(l) is mono- or dinuclear.

3.2. Structures of 1 and 2. The overall description of the crystal structures and the packing of the ions in **1**, **2**, and **3** has been presented in the Supporting Information, Section S3. The following discussion concentrates on the structures of [AgD₆]⁺ cation complexes and the changes in the D₆ molecules upon complexation. The structures of [AgD₆]⁺ in both **1** and **2** (see Figure 1) are similar but that in **1** more closely resembles the ideal D_{6h} symmetric structure, in which Ag⁺ is at the center of the plane of the fully symmetrical Si₆O₆ ring. However [AgD₆]⁺ in **1** is better described as having a D_{3h} symmetry since all of the oxygen atoms are not equally coordinated to Ag⁺. Three of the oxygen atoms (see Table 3) in the Si₆O₆ ring are more strongly coordinating toward silver(I) (avg. Ag...O contact 2.422(5), 0.208 v.u.) than the other three oxygen atoms (avg. Ag...O contact 2.656(5), 0.110 v.u.). The strongly and weakly coordinating oxygens are *trans* to one another. In **2**, Ag⁺ is slipped even further from the center of the plane of the Si₆O₆ ring and there is no significant coordination between Ag⁺ and O2 atoms (3.069(4) Å, 0.036 v.u.,⁴¹ c.f. sum of the silver and oxygen van der Waals radii of 3.27 Å). The other five silver(I) oxygen contacts range from 2.419(4) to 2.798(6) Å. The distortion results from a Ag^{δ+}...F^{δ-} cation anion interaction, which is greater in the more basic [FAl{OC(CF₃)₃}₃]⁻ salt (0.041 v.u. vs

0.267 v.u.) leading to a displacement of Ag⁺ above the Si₆O₆ plane in **2** (1.221(4) Å), and a markedly stronger coordination to oxygen atoms in **1** (0.954 v.u.) than in **2** (0.604 v.u.). The Ag^{δ+}...F^{δ-} interaction in **2** is similar in strength to that found between [FAl{OC(CF₃)₃}₃]^{δ-} unit and one of the Li^{δ+} atoms in (SO₂)₂Li[AlF{OC(CF₃)₃}₃Li[Al{OC(CF₃)₃}₄]] (1.845(5) Å, 0.268 v.u.).⁴² The sum of the bond valences of the metal oxygen contacts indicates a stronger coordination between M⁺ (M = Li, Ag) and D_n (n = 6, 7) in **1** (0.954 v.u.) than in [LiD₆][Al{OC(CF₃)₃}₄] (0.810 v.u.)⁸ or [AgD₇][SbF₆] (0.629 v.u.)¹⁰ (See Table 3). This suggests that in the solid state, Ag⁺ is a stronger Lewis acid than Li⁺ toward D₆, while D₆ is a stronger base than D₇ toward Ag⁺. The sum of the bond valences (**1** 1.023 v.u.; **2** 0.907 v.u.) of all Ag-O contacts and Ag-F contacts correspond to one positive charge on silver.

The M06-L/6-311++G(2d,p) optimized structure of [AgD₆]⁺ presented in Figure 2 deviates even further from the ideal D_{6h} symmetry than the approximately D_{3h} symmetric experimental structure in **1** by distorting the Si₆O₆ ring and moving the silver(I) atom away from the plane of the ring resulting in an overall symmetry of C₃. The ideal D_{6h} symmetric structure is calculated to be a saddle point on the potential energy surface lying +18.4 kJ mol⁻¹ higher in energy than the minimum structure (+11.4 kJ mol⁻¹ at RI-MP2/def2-TZVPP level of theory).⁴³ The difference between the Ag-O1 and Ag-O2 contacts in the optimized structure (Figure 2) is also larger than the differences between the opposite Ag-O contacts in the Si₆O₆ rings of **1** (Figure 1), making the optimized ring more distorted from the ideal D_{6h} symmetry than the experimental structure. The calculated structure is reminiscent of the [AgD₆]⁺ in **2** where the silver(I) atom lies above the Si₆O₆ ring. It is presumed that the two weak Ag(I)...F contacts are enough to stabilize the more symmetric planar structure observed in **1** over the less symmetric gas phase structure. In **2**, with only one fluorine contact to the silver(I), the gas phase structure is retained.

Previously neutral D₆ has been determined by electron diffraction to have a D_{3d} symmetric structure, where the Si₆O₆ ring is puckered with all oxygen atoms forming a plane and silicon atoms lying alternately above and below the plane with some methyl groups pointing inward.⁴⁴ However our calculations predict a lower symmetry puckered C_i structure (See Figure 3) as the minimum structure for D₆ instead of the D_{3d} structure. The discrepancy might arise from the fact that the electron diffraction study⁴⁴ only considered higher symmetries (C_{6v}, D_{3d}, S₆, and C₆) for fitting the D₆ structural data based on evidence from an earlier vibrational study.⁴⁷ Furthermore the authors of the electron diffraction study did admit that the experimental conformation of D₆ was ill-defined. Another study⁴⁸ had suggested that the solid state structure of D₆ should resemble that of the chair conformation in N₆P₆(NMe₂)₁₂ (See Supporting Information, Figure S3.8),⁴⁹ and our optimized structure of D₆ does bear a certain resemblance to that of N₆P₆(NMe₂)₁₂. The more symmetrical D_{3d} structure of D₆ is calculated to be a saddle point +67.5 kJ mol⁻¹ higher in energy than the minimum structure (energy difference of the structures at the RI-MP2/def2-TZVPP level of theory +19.0 kJ mol⁻¹).⁴³

Compared to the puckered (calculated) structure of neutral D₆ the Si₆O₆ framework in **1** and **2** is nearly planar similar to the structures of the lithium complexes [LiD₆][Al{OC(CF₃)₂Ph}₄] and [LiD₆][Al{OC(CF₃)₃}₄] (see Figure 3).⁸ In [LiD₆]⁺ complexes the D₆ ring is more distorted from the ideal

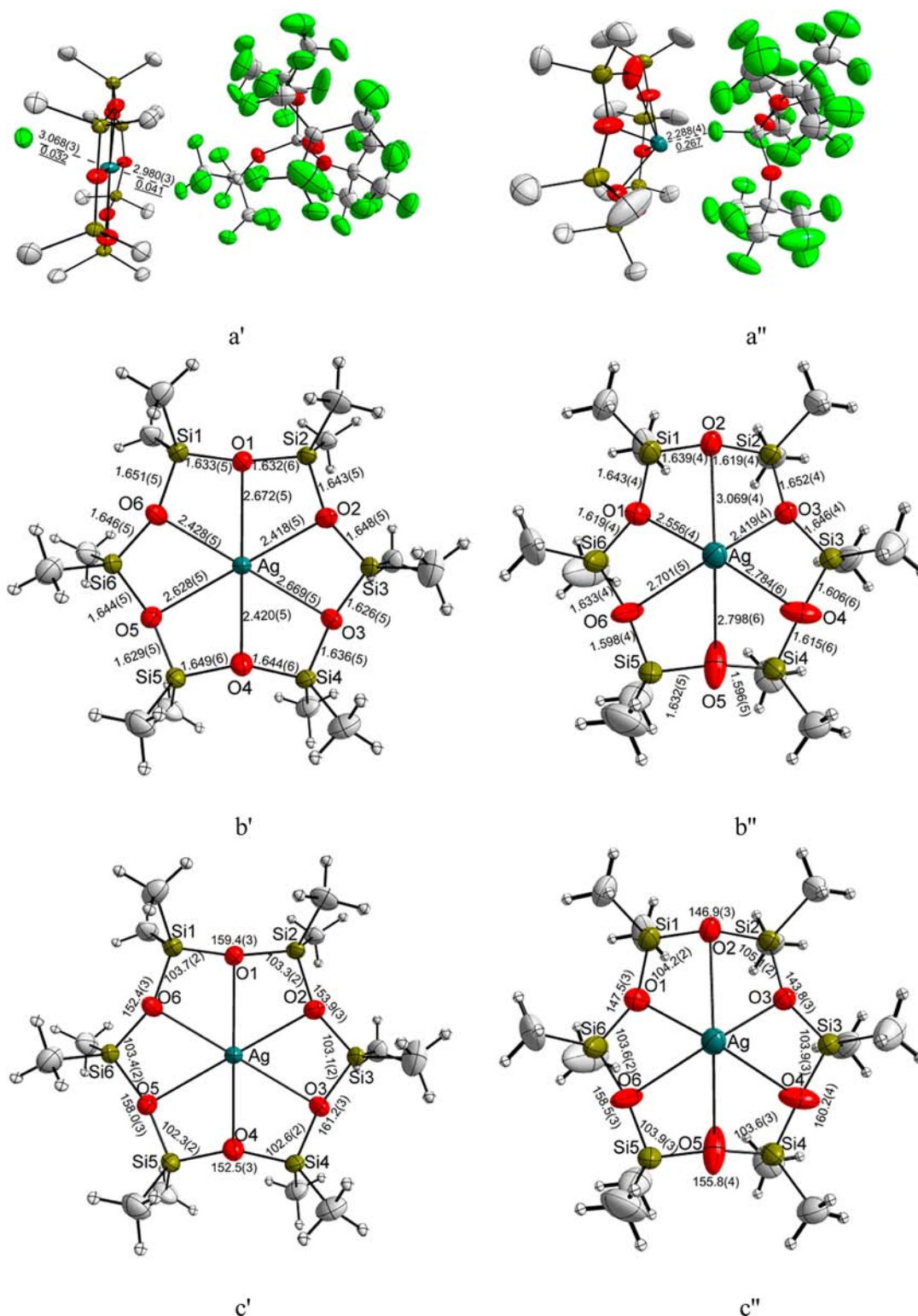


Figure 1. (a) Closest silver(I)-anion contacts (bond valences [v.u.]),⁴¹ (b) bond lengths [Å], and (c) bond angles [deg] in **1** (') and **2** ("). Thermal ellipsoids drawn at 50% probability level.

D_{6h} symmetric structure than the D_6 rings in **1** and **2**. In the $[\text{LiD}_6]^+$ complex structures four of the D_6 oxygen atoms are coordinated more strongly to Li^+ than the other two (c.f. avg. $\text{Ag}\cdots\text{O}_c$ contacts 2.052(20) Å and $\text{Ag}\cdots\text{O}_{wc}$ contacts 3.248(20) Å, respectively in $[\text{LiD}_6][\text{Al}\{\text{OC}(\text{CF}_3)_3\}_4]$.⁸ The difference between the strong and weak metal oxygen contacts is larger in $[\text{LiD}_6]^+$ than in $[\text{AgD}_6]^+$ complexes (c.f. avg. $\text{Ag}\cdots\text{O}_c$ contacts

2.591(5) Å and $\text{Ag}\cdots\text{O}_{wc}$ contacts 2.851(5) Å, respectively in **1**). The average bond lengths between the silicon and oxygen atoms coordinated to metal ions $\text{O}_c\text{-Si}$ become longer in all complexes [see Table 3, for example, avg. $\text{O}_c\text{-Si}$ 1.647(5) Å in **1** and avg. $\text{O}_c\text{-Si}$ 1.658(7) Å in $[\text{LiD}_6][\text{Al}\{\text{OC}(\text{CF}_3)_3\}_4]$ compared to those in free D_6 (O-Si 1.622(1) Å).⁴⁴ The effect is more pronounced for the lithium complexes. In contrast, the

Table 3. Average Structural Parameters of the Experimental and Calculated (M06-L/6-311++G(2d,p)) D₆ and 18-crown-6 Complexes of Lithium and Silver(I) and Those of [AgD₇][SbF₆]

	avg. M–O [Range], $\Sigma_{i,j,u}$	O–Si	avg. O–X [Range]	Si–O–Si	avg. X–O–X [Range]
D ₆ ^a (Exptl. D _{3d})		O–Si	1.622(1)	Si–O–Si	149.6(1)
D ₆ (Calc. D _{3d})		O–Si	1.627	Si–O–Si	167.9
D ₆ (Calc. C _i)		O–Si	1.640 [1.636–1.646]	Si–O–Si	137.2 [130.4–144.1]
[AgD ₆][Al(OR _p) ₄] (1)	Ag–O _c	O _c –Si	1.647 [1.643(S)–1.651(S)]	Si–O _c –Si	152.9 [152.4(3)–153.9(3)]
	Ag–O _{wc}	O _{wc} –Si	1.656 [2.628(S)–2.672(S)], 0.331	Si–O _{wc} –Si	159.5 [158.0(3)–161.2(3)]
[AgD ₆][AlF(OR _p) ₃] (2)	Ag–O _c	O _c –Si	1.631 [1.596(S)–1.652(4)]	Si–O _c –Si	149.0 [143.8(3)–155.8(4)]
	Ag–O _{wc}	O _{wc} –Si	1.618 [1.598(4)–1.639(4)]	Si–O _{wc} –Si	155.2 [146.9(3)–160.2(4)]
[AgD ₆] ⁺ (Calc. C _s)	Ag–O _c	O _c –Si	1.669	Si–O _c –Si	142.2
	Ag–O _{wc}	O _{wc} –Si	1.646	Si–O _{wc} –Si	144.5
[AgD ₇][SbF ₆] ^b	Ag–O _c	O _c –Si	1.636 [1.626(1)–1.647(1)]	Si–O _c –Si	144.1 [138.7(1)–148.4(1)]
	Ag–O _{wc}	O _{wc} –Si	1.608 [1.605(1)–1.611(1)]	Si–O _{wc} –Si	166.9(1)
[LiD ₆][Al(OR _p) ₄] ^c	Li–O _c	O _c –Si	1.658 [1.645(7)–1.671(7)]	Si–O _c –Si	141.0 [139.6(4)–141.9(4)]
	Li–O _{wc}	O _{wc} –Si	1.625 [1.607(8)–1.633(8)]	Si–O _{wc} –Si	148.3 [146.1(5)–150.4(5)]
[LiD ₆] ⁺ (Calc. C _s)	Li–O _c	O _c –Si	1.670 [1.661–1.679]	Si–O _c –Si	139.3
	Li–O _{wc}	O _{wc} –Si	1.638 [1.636–1.639]	Si–O _{wc} –Si	135.8
(18-crown-6) (Exptl. C _i) ^d	Ag–O _c	O _c –C	1.423 [1.418(1)–1.430(1)]	C–O–C	112.8 [112.7(1)–113.0(1)]
(18-crown-6) (Calc. C _i)	Ag–O _{wc}	O _{wc} –C	1.410 [1.406–1.417]	C–O–C	113.8 [112.9–114.6]
(18-crown-6) (Calc. D _{3d})	Ag–O _{ax}	O _{ax} –C	1.406	C–O–C	112.1
[Ag(18-crown-6)] ₂ [SbF ₆] ₂ (3)	Ag–O _c	O _c –C	1.427 [1.424(S)–1.429(4)]	C–O _c –C	111.8 [111.2(2)–112.4(2)]
	Ag–O _{wc}	O _{wc} –C	1.429 [1.427(4)–1.431(S)]	C–O _{wc} –C	112.7 [112.1(2)–113.2(3)]
	Ag–O _{ax}	O _{ax} –C	1.435 [1.434(4)–1.436(4)]		
[Ag(18-crown-6)] ⁺ (Calc. C ₂)	Ag–O	O–C	1.424 [1.419–1.426]	C–O–C	113.3 [113.1–113.4]
[Ag(18-crown-6)] ₂ ²⁺ (Calc. C _i)	Ag–O _c	O _c –C	1.422 [1.419–1.425]	C–O _c –C	112.5 [111.7–113.4]
	Ag–O _{wc}	O _{wc} –C	1.426 [1.425–1.426]	C–O _{wc} –C	111.8 [111.4–112.1]
	Ag–O _{ax}	O _{ax} –C	1.432 [1.431–1.432]		
[Li(18-crown-6)] ⁺ (Calc. D ₂)	Li–O	O–C	1.422 [1.416–1.427]	C–O–C	114.8 [114.0–116.6]
[Li(18-crown-6)][Nd ^{III}] ^e	Li–O	O–C	1.404 [1.366(10)–1.462(8)]	C–O–C	114.6 [112.1(S)–119.7(6)]

^aRef 44. ^bRef 10. ^cRef 8. ^dRef 45. ^eRef 45. ^fRef 45. ^gRef 45. ^hRef 45. ⁱRef 45. ^jRef 45. ^kRef 45. ^lRef 45. ^mRef 45. ⁿRef 45. ^oRef 45. ^pRef 45. ^qRef 45. ^rRef 45. ^sRef 45. ^tRef 45. ^uRef 45. ^vRef 45. ^wRef 45. ^xRef 45. ^yRef 45. ^zRef 45. ^{aa}Ref 45. ^{ab}Ref 45. ^{ac}Ref 45. ^{ad}Ref 45. ^{ae}Ref 45. ^{af}Ref 45. ^{ag}Ref 45. ^{ah}Ref 45. ^{ai}Ref 45. ^{aj}Ref 45. ^{ak}Ref 45. ^{al}Ref 45. ^{am}Ref 45. ^{an}Ref 45. ^{ao}Ref 45. ^{ap}Ref 45. ^{aq}Ref 45. ^{ar}Ref 45. ^{as}Ref 45. ^{at}Ref 45. ^{au}Ref 45. ^{av}Ref 45. ^{aw}Ref 45. ^{ax}Ref 45. ^{ay}Ref 45. ^{az}Ref 45. ^{ba}Ref 45. ^{bb}Ref 45. ^{bc}Ref 45. ^{bd}Ref 45. ^{be}Ref 45. ^{bf}Ref 45. ^{bg}Ref 45. ^{bh}Ref 45. ^{bi}Ref 45. ^{bj}Ref 45. ^{bk}Ref 45. ^{bl}Ref 45. ^{bm}Ref 45. ^{bn}Ref 45. ^{bo}Ref 45. ^{bp}Ref 45. ^{bq}Ref 45. ^{br}Ref 45. ^{bs}Ref 45. ^{bt}Ref 45. ^{bu}Ref 45. ^{bv}Ref 45. ^{bw}Ref 45. ^{bx}Ref 45. ^{by}Ref 45. ^{bz}Ref 45. ^{ca}Ref 45. ^{cb}Ref 45. ^{cc}Ref 45. ^{cd}Ref 45. ^{ce}Ref 45. ^{cf}Ref 45. ^{cg}Ref 45. ^{ch}Ref 45. ^{ci}Ref 45. ^{cj}Ref 45. ^{ck}Ref 45. ^{cl}Ref 45. ^{cm}Ref 45. ^{cn}Ref 45. ^{co}Ref 45. ^{cp}Ref 45. ^{cq}Ref 45. ^{cr}Ref 45. ^{cs}Ref 45. ^{ct}Ref 45. ^{cu}Ref 45. ^{cv}Ref 45. ^{cw}Ref 45. ^{cx}Ref 45. ^{cy}Ref 45. ^{cz}Ref 45. ^{da}Ref 45. ^{db}Ref 45. ^{dc}Ref 45. ^{dd}Ref 45. ^{de}Ref 45. ^{df}Ref 45. ^{dg}Ref 45. ^{dh}Ref 45. ^{di}Ref 45. ^{dj}Ref 45. ^{dk}Ref 45. ^{dl}Ref 45. ^{dm}Ref 45. ^{dn}Ref 45. ^{do}Ref 45. ^{dp}Ref 45. ^{dq}Ref 45. ^{dr}Ref 45. ^{ds}Ref 45. ^{dt}Ref 45. ^{du}Ref 45. ^{dv}Ref 45. ^{dw}Ref 45. ^{dx}Ref 45. ^{dy}Ref 45. ^{dz}Ref 45. ^{ea}Ref 45. ^{eb}Ref 45. ^{ec}Ref 45. ^{ed}Ref 45. ^{ee}Ref 45. ^{ef}Ref 45. ^{eg}Ref 45. ^{eh}Ref 45. ^{ei}Ref 45. ^{ej}Ref 45. ^{ek}Ref 45. ^{el}Ref 45. ^{em}Ref 45. ^{en}Ref 45. ^{eo}Ref 45. ^{ep}Ref 45. ^{eq}Ref 45. ^{er}Ref 45. ^{es}Ref 45. ^{et}Ref 45. ^{eu}Ref 45. ^{ev}Ref 45. ^{ew}Ref 45. ^{ex}Ref 45. ^{ey}Ref 45. ^{ez}Ref 45. ^{fa}Ref 45. ^{fb}Ref 45. ^{fc}Ref 45. ^{fd}Ref 45. ^{fe}Ref 45. ^{ff}Ref 45. ^{fg}Ref 45. ^{fh}Ref 45. ^{fi}Ref 45. ^{fj}Ref 45. ^{fk}Ref 45. ^{fl}Ref 45. ^{fm}Ref 45. ^{fn}Ref 45. ^{fo}Ref 45. ^{fp}Ref 45. ^{fq}Ref 45. ^{fr}Ref 45. ^{fs}Ref 45. ^{ft}Ref 45. ^{fu}Ref 45. ^{fv}Ref 45. ^{fw}Ref 45. ^{fx}Ref 45. ^{fy}Ref 45. ^{fz}Ref 45. ^{ga}Ref 45. ^{gb}Ref 45. ^{gc}Ref 45. ^{gd}Ref 45. ^{ge}Ref 45. ^{gf}Ref 45. ^{gg}Ref 45. ^{gh}Ref 45. ^{gi}Ref 45. ^{gj}Ref 45. ^{gk}Ref 45. ^{gl}Ref 45. ^{gm}Ref 45. ^{gn}Ref 45. ^{go}Ref 45. ^{gp}Ref 45. ^{gq}Ref 45. ^{gr}Ref 45. ^{gs}Ref 45. ^{gt}Ref 45. ^{gu}Ref 45. ^{gv}Ref 45. ^{gw}Ref 45. ^{gx}Ref 45. ^{gy}Ref 45. ^{gz}Ref 45. ^{ha}Ref 45. ^{hb}Ref 45. ^{hc}Ref 45. ^{hd}Ref 45. ^{he}Ref 45. ^{hf}Ref 45. ^{hg}Ref 45. ^{hh}Ref 45. ^{hi}Ref 45. ^{hj}Ref 45. ^{hk}Ref 45. ^{hl}Ref 45. ^{hm}Ref 45. ^{hn}Ref 45. ^{ho}Ref 45. ^{hp}Ref 45. ^{hq}Ref 45. ^{hr}Ref 45. ^{hs}Ref 45. ^{ht}Ref 45. ^{hu}Ref 45. ^{hv}Ref 45. ^{hw}Ref 45. ^{hx}Ref 45. ^{hy}Ref 45. ^{hz}Ref 45. ^{ia}Ref 45. ^{ib}Ref 45. ^{ic}Ref 45. ^{id}Ref 45. ^{ie}Ref 45. ^{if}Ref 45. ^{ig}Ref 45. ^{ih}Ref 45. ⁱⁱRef 45. ^{ij}Ref 45. ^{ik}Ref 45. ^{il}Ref 45. ^{im}Ref 45. ⁱⁿRef 45. ^{io}Ref 45. ^{ip}Ref 45. ^{iq}Ref 45. ^{ir}Ref 45. ^{is}Ref 45. ^{it}Ref 45. ^{iu}Ref 45. ^{iv}Ref 45. ^{iw}Ref 45. ^{ix}Ref 45. ^{iy}Ref 45. ^{iz}Ref 45. ^{ja}Ref 45. ^{jb}Ref 45. ^{jc}Ref 45. ^{jd}Ref 45. ^{je}Ref 45. ^{jf}Ref 45. ^{jj}Ref 45. ^{kg}Ref 45. ^{kh}Ref 45. ^{ki}Ref 45. ^{kj}Ref 45. ^{kk}Ref 45. ^{kl}Ref 45. ^{km}Ref 45. ^{kn}Ref 45. ^{ko}Ref 45. ^{kp}Ref 45. ^{kq}Ref 45. ^{kr}Ref 45. ^{ks}Ref 45. ^{kt}Ref 45. ^{ku}Ref 45. ^{kv}Ref 45. ^{kw}Ref 45. ^{kx}Ref 45. ^{ky}Ref 45. ^{kz}Ref 45. ^{la}Ref 45. ^{lb}Ref 45. ^{lc}Ref 45. ^{ld}Ref 45. ^{le}Ref 45. ^{lf}Ref 45. ^{lg}Ref 45. ^{lh}Ref 45. ^{li}Ref 45. ^{lj}Ref 45. ^{lk}Ref 45. ^{lm}Ref 45. ^{ln}Ref 45. ^{lo}Ref 45. ^{lp}Ref 45. ^{lq}Ref 45. ^{lr}Ref 45. ^{ls}Ref 45. ^{lt}Ref 45. ^{lu}Ref 45. ^{lv}Ref 45. ^{lw}Ref 45. ^{lx}Ref 45. ^{ly}Ref 45. ^{lz}Ref 45. ^{ma}Ref 45. ^{mb}Ref 45. ^{mc}Ref 45. ^{md}Ref 45. ^{me}Ref 45. ^{mf}Ref 45. ^{mg}Ref 45. ^{mh}Ref 45. ^{mi}Ref 45. ^{mj}Ref 45. ^{mk}Ref 45. ^{ml}Ref 45. ^{mn}Ref 45. ^{mo}Ref 45. ^{mp}Ref 45. ^{mq}Ref 45. ^{mr}Ref 45. ^{ms}Ref 45. ^{mt}Ref 45. ^{mu}Ref 45. ^{mv}Ref 45. ^{mw}Ref 45. ^{mx}Ref 45. ^{my}Ref 45. ^{mz}Ref 45. ^{na}Ref 45. ^{nb}Ref 45. ^{nc}Ref 45. ndRef 45. ^{ne}Ref 45. ^{nf}Ref 45. ^{ng}Ref 45. ^{nh}Ref 45. ⁿⁱRef 45. ^{nj}Ref 45. ^{nk}Ref 45. ^{nl}Ref 45. ^{no}Ref 45. ^{np}Ref 45. ^{nq}Ref 45. ^{nr}Ref 45. ^{ns}Ref 45. ^{nt}Ref 45. ^{nu}Ref 45. ^{nv}Ref 45. ^{nw}Ref 45. ^{nx}Ref 45. ^{ny}Ref 45. ^{nz}Ref 45. ^{oa}Ref 45. ^{ob}Ref 45. ^{oc}Ref 45. ^{od}Ref 45. ^{oe}Ref 45. ^{of}Ref 45. ^{og}Ref 45. ^{oh}Ref 45. ^{oi}Ref 45. ^{oj}Ref 45. ^{ok}Ref 45. ^{ol}Ref 45. ^{om}Ref 45. ^{on}Ref 45. ^{oo}Ref 45. ^{op}Ref 45. ^{oq}Ref 45. ^{or}Ref 45. ^{os}Ref 45. ^{ot}Ref 45. ^{ou}Ref 45. ^{ov}Ref 45. ^{ow}Ref 45. ^{ox}Ref 45. ^{oy}Ref 45. ^{oz}Ref 45. ^{pa}Ref 45. ^{pb}Ref 45. ^{pc}Ref 45. ^{pd}Ref 45. ^{pe}Ref 45. ^{pf}Ref 45. ^{pg}Ref 45. ^{ph}Ref 45. ^{pi}Ref 45. ^{pj}Ref 45. ^{pk}Ref 45. ^{pl}Ref 45. ^{pm}Ref 45. ^{pn}Ref 45. ^{po}Ref 45. ^{pp}Ref 45. ^{pq}Ref 45. ^{pr}Ref 45. ^{ps}Ref 45. ^{pt}Ref 45. ^{pu}Ref 45. ^{pv}Ref 45. ^{pw}Ref 45. ^{px}Ref 45. ^{py}Ref 45. ^{pz}Ref 45. ^{qa}Ref 45. ^{qb}Ref 45. ^{qc}Ref 45. ^{qd}Ref 45. ^{qe}Ref 45. ^{qf}Ref 45. ^{qg}Ref 45. ^{qh}Ref 45. ^{qi}Ref 45. ^{qj}Ref 45. ^{qk}Ref 45. ^{ql}Ref 45. ^{qm}Ref 45. ^{qn}Ref 45. ^{qo}Ref 45. ^{qp}Ref 45. ^{qq}Ref 45. ^{qr}Ref 45. ^{qs}Ref 45. ^{qt}Ref 45. ^{qu}Ref 45. ^{qv}Ref 45. ^{qw}Ref 45. ^{qx}Ref 45. ^{qy}Ref 45. ^{qz}Ref 45. ^{ra}Ref 45. ^{rb}Ref 45. ^{rc}Ref 45. rdRef 45. ^{re}Ref 45. ^{rf}Ref 45. ^{rg}Ref 45. ^{rh}Ref 45. ^{ri}Ref 45. ^{rj}Ref 45. ^{rk}Ref 45. ^{rl}Ref 45. ^{rm}Ref 45. ^{rn}Ref 45. ^{ro}Ref 45. ^{rp}Ref 45. ^{rq}Ref 45. ^{rr}Ref 45. ^{rs}Ref 45. ^{rt}Ref 45. ^{ru}Ref 45. ^{rv}Ref 45. ^{rw}Ref 45. ^{rx}Ref 45. ^{ry}Ref 45. ^{rz}Ref 45. ^{sa}Ref 45. ^{sb}Ref 45. ^{sc}Ref 45. ^{sd}Ref 45. ^{se}Ref 45. ^{sf}Ref 45. ^{sg}Ref 45. ^{sh}Ref 45. ^{si}Ref 45. ^{sj}Ref 45. ^{sk}Ref 45. ^{sl}Ref 45. smRef 45. ^{sn}Ref 45. ^{so}Ref 45. ^{sp}Ref 45. ^{sq}Ref 45. ^{sr}Ref 45. ^{ss}Ref 45. stRef 45. ^{su}Ref 45. ^{sv}Ref 45. ^{sw}Ref 45. ^{sx}Ref 45. ^{sy}Ref 45. ^{sz}Ref 45. ^{ta}Ref 45. ^{tb}Ref 45. ^{tc}Ref 45. ^{td}Ref 45. ^{te}Ref 45. ^{tf}Ref 45. ^{tg}Ref 45. thRef 45. ^{ti}Ref 45. ^{tj}Ref 45. ^{tk}Ref 45. ^{tl}Ref 45. tmRef 45. ^{tn}Ref 45. ^{to}Ref 45. ^{tp}Ref 45. ^{tq}Ref 45. ^{tr}Ref 45. ^{ts}Ref 45. ^{tu}Ref 45. ^{tv}Ref 45. ^{tw}Ref 45. ^{tx}Ref 45. ^{ty}Ref 45. ^{tz}Ref 45. ^{ua}Ref 45. ^{ub}Ref 45. ^{uc}Ref 45. ^{ud}Ref 45. ^{ue}Ref 45. ^{uf}Ref 45. ^{ug}Ref 45. ^{uh}Ref 45. ^{ui}Ref 45. ^{uj}Ref 45. ^{uk}Ref 45. ^{ul}Ref 45. ^{um}Ref 45. ^{un}Ref 45. ^{uo}Ref 45. ^{up}Ref 45. ^{uq}Ref 45. ^{ur}Ref 45. ^{us}Ref 45. ^{ut}Ref 45. ^{uu}Ref 45. ^{uv}Ref 45. ^{uw}Ref 45. ^{ux}Ref 45. ^{uy}Ref 45. ^{uz}Ref 45. ^{va}Ref 45. ^{vb}Ref 45. ^{vc}Ref 45. ^{vd}Ref 45. ^{ve}Ref 45. ^{vf}Ref 45. ^{vg}Ref 45. ^{vh}Ref 45. ^{vi}Ref 45. ^{vj}Ref 45. ^{vk}Ref 45. ^{vl}Ref 45. ^{vm}Ref 45. ^{vn}Ref 45. ^{vo}Ref 45. ^{vp}Ref 45. ^{vq}Ref 45. ^{vr}Ref 45. ^{vs}Ref 45. ^{vt}Ref 45. ^{vu}Ref 45. ^{vv}Ref 45. ^{vw}Ref 45. ^{vx}Ref 45. ^{vy}Ref 45. ^{vz}Ref 45. ^{wa}Ref 45. ^{wb}Ref 45. ^{wc}Ref 45. ^{wd}Ref 45. ^{we}Ref 45. ^{wf}Ref 45. ^{wg}Ref 45. ^{wh}Ref 45. ^{wi}Ref 45. ^{wj}Ref 45. ^{wk}Ref 45. ^{wl}Ref 45. ^{wm}Ref 45. ^{wn}Ref 45. ^{wo}Ref 45. ^{wp}Ref 45. ^{wq}Ref 45. ^{wr}Ref 45. ^{ws}Ref 45. ^{wt}Ref 45. ^{wu}Ref 45. ^{wv}Ref 45. ^{ww}Ref 45. ^{wx}Ref 45. ^{wy}Ref 45. ^{wz}Ref 45. ^{xa}Ref 45. ^{xb}Ref 45. ^{xc}Ref 45. ^{xd}Ref 45. ^{xe}Ref 45. ^{xf}Ref 45. ^{xg}Ref 45. ^{xh}Ref 45. ^{xi}Ref 45. ^{xj}Ref 45. ^{xk}Ref 45. ^{xl}Ref 45. ^{xm}Ref 45. ^{xn}Ref 45. ^{xo}Ref 45. ^{xp}Ref 45. ^{xq}Ref 45. ^{xr}Ref 45. ^{xs}Ref 45. ^{xt}Ref 45. ^{xu}Ref 45. ^{xv}Ref 45. ^{xw}Ref 45. ^{xx}Ref 45. ^{xy}Ref 45. ^{xz}Ref 45. ^{ya}Ref 45. ^{yb}Ref 45. ^{yc}Ref 45. ^{yd}Ref 45. ^{ye}Ref 45. ^{yf}Ref 45. ^{yg}Ref 45. ^{yh}Ref 45. ^{yi}Ref 45. ^{yj}Ref 45. ^{yk}Ref 45. ^{yl}Ref 45. ^{ym}Ref 45. ^{yn}Ref 45. ^{yo}Ref 45. ^{yp}Ref 45. ^{yq}Ref 45. ^{yr}Ref 45. ^{ys}Ref 45. ^{yt}Ref 45. ^{yu}Ref 45. ^{yv}Ref 45. ^{yw}Ref 45. ^{yx}Ref 45. ^{yy}Ref 45. ^{yz}Ref 45. ^{za}Ref 45. ^{zb}Ref 45. ^{zc}Ref 45. ^{zd}Ref 45. ^{ze}Ref 45. ^{zf}Ref 45. ^{zg}Ref 45. ^{zh}Ref 45. ^{zi}Ref 45. ^{zj}Ref 45. ^{zk}Ref 45. ^{zl}Ref 45. ^{zm}Ref 45. ^{zn}Ref 45. ^{zo}Ref 45. ^{zp}Ref 45. ^{zq}Ref 45. ^{zr}Ref 45. ^{zs}Ref 45. ^{zt}Ref 45. ^{zu}Ref 45. ^{zv}Ref 45. ^{zw}Ref 45. ^{zx}Ref 45. ^{zy}Ref 45. ^{zz}Ref 45. ^{aa}Ref 45. ^{ab}Ref 45. ^{ac}Ref 45. ^{ad}Ref 45. ^{ae}Ref 45. ^{af}Ref 45. ^{ag}Ref 45. ^{ah}Ref 45. ^{ai}Ref 45. ^{aj}Ref 45. ^{ak}Ref 45. ^{al}Ref 45. ^{am}Ref 45. ^{an}Ref 45. ^{ao}Ref 45. ^{ap}Ref 45. ^{aq}Ref 45. ^{ar}Ref 45. ^{as}Ref 45. ^{at}Ref 45. ^{au}Ref 45. ^{av}Ref 45. ^{aw}Ref 45. ^{ax}Ref 45. ^{ay}Ref 45. ^{az}Ref 45. ^{ba}Ref 45. ^{bb}Ref 45. ^{bc}Ref 45. ^{bd}Ref 45. ^{be}Ref 45. ^{bf}Ref 45. ^{bg}Ref 45. ^{bh}Ref 45. ^{bi}Ref 45. ^{bj}Ref 45. ^{bk}Ref 45. ^{bl}Ref 45. ^{bm}Ref 45. ^{bn}Ref 45. ^{bo}Ref 45. ^{bp}Ref 45. ^{bq}Ref 45. ^{br}Ref 45. ^{bs}Ref 45. ^{bt}Ref 45. ^{bu}Ref 45. ^{bv}Ref 45. ^{bw}Ref 45. ^{bx}Ref 45. ^{by}Ref 45. ^{bz}Ref 45. ^{ca}Ref 45. ^{cb}Ref 45. ^{cc}Ref 45. ^{cd}Ref 45. ^{ce}Ref 45. ^{cf}Ref 45. ^{cg}Ref 45. ^{ch}Ref 45. ^{ci}Ref 45. ^{cj}Ref 45. ^{ck}Ref 45. ^{cl}Ref 45. ^{cm}Ref 45. ^{cn}Ref 45. ^{co}Ref 45. ^{cp}Ref 45. ^{cq}Ref 45. ^{cr}Ref 45. ^{cs}Ref 45. ^{ct}Ref 45. ^{cu}Ref 45. ^{cv}Ref 45. ^{cw}Ref 45. ^{cx}Ref 45. ^{cy}Ref 45.

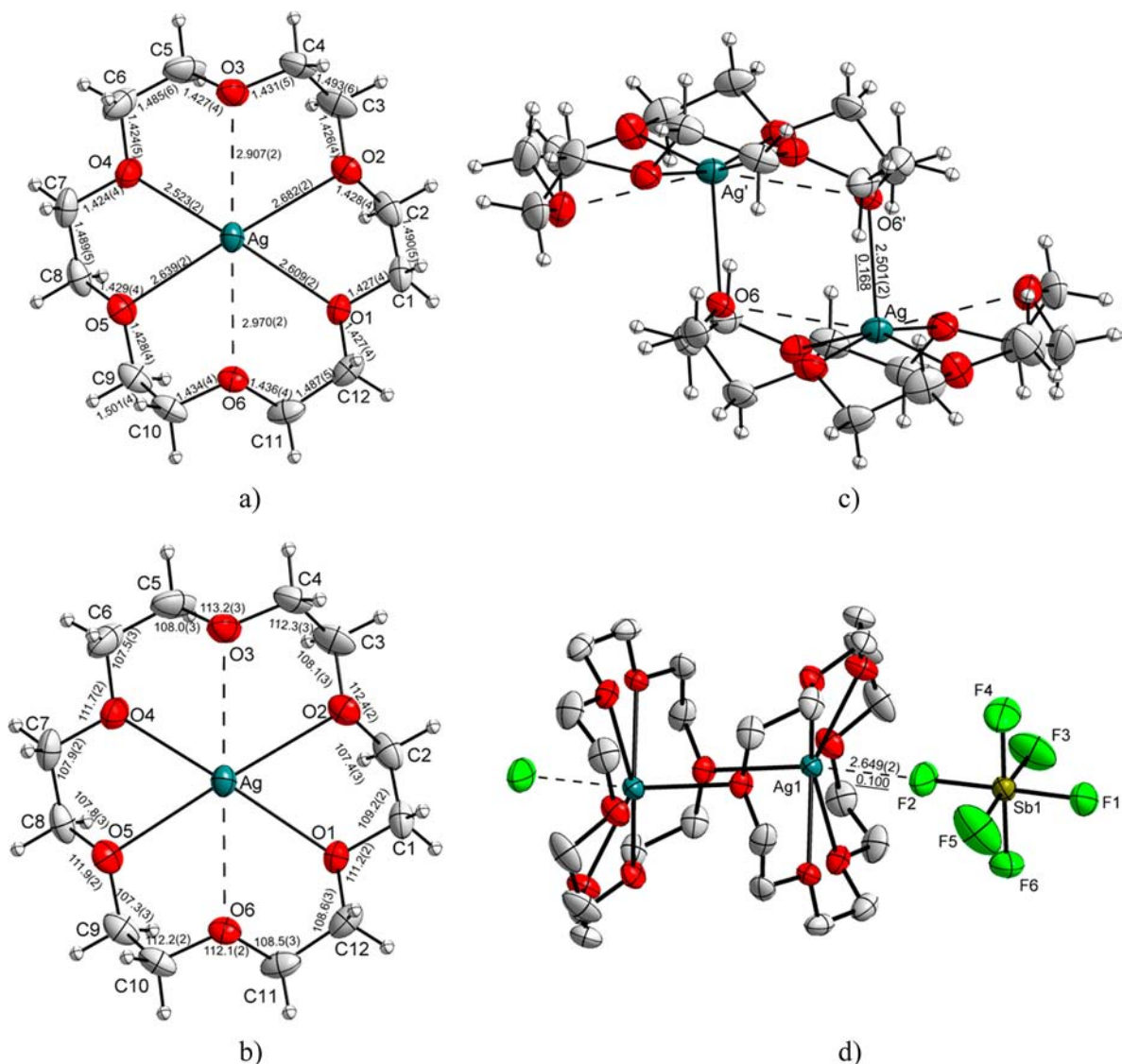


Figure 4. Top-view of one-half of $[\text{Ag}(\text{18-crown-6})]_2^{2+}$ with (a) bond lengths [Å] and (b) bond angles [deg]. (c) A side-view of $[\text{Ag}(\text{18-crown-6})]_2^{2+}$ with intradimer Ag–O contacts [Å and v.u.]. (d) Cation–anion contacts in $[\text{SbF}_6]^- \cdots [\text{Ag}(\text{18-crown-6})]_2^{2+} \cdots [\text{SbF}_6]^-$ ion pair of **3**. Thermal ellipsoids have been drawn at 50% probability.

calculated dinuclear $[\text{Ag}(\text{18-crown-6})]_2^{2+}$ complex are in good agreement with the structure of **3** (see Table 3) albeit most of the silver(I) oxygen contacts are calculated shorter than those in the observed structure (e.g., avg. Ag–O_c 2.577 Å calc. vs 2.613(2) Å exptl.). It appears that while an 18-crown-6 ring distorts to give a stronger binding to silver(I) the formation of the dinuclear complex is favored over the more extended distortion of the ring exhibited by the mononuclear complex. Furthermore the formation of the dinuclear complex appears to be more favorable in the solid state than filling the silver coordination environment with stronger anion contacts from $[\text{SbF}_6]^-$. Since the sum of the Ag \cdots O bond valences from one 18-crown-6 ring in **3** (0.604 v.u.) is less than those in **1** (0.954 v.u.) and **2** (0.640 v.u.) it might be tempting to think that 18-crown-6 acts as weaker base toward Ag⁺ in the solid state than D₆. However, the lower bond valence sum is more likely an indirect result of the coordination from the second 18-crown-6 ring and the more coordinating anion in **3**.

The optimized structure of $[\text{Li}(\text{18-crown-6})]^+$ exhibits a similar folded ring around the lithium atom to that found, for

example, in the crystal structure of $[\text{Li}(\text{18-crown-6})][\text{Nd}(\eta^5\text{-Cp}^*)_2(\kappa^1\text{-O}_3\text{SCF}_3)(\kappa^2\text{-O}_3\text{SCF}_3)]^{46}$ (see Table 3 and Supporting Information, Figure S4.1). The optimized folded ring structure of $[\text{Li}(\text{18-crown-6})]^+$ is also in agreement with the optimized minimum conformation reported for the complex in previous studies.⁵¹ Because of the relatively small size of lithium compared to that of the 18-crown-6 ring, crystal structures where lithium is asymmetrically coordinated to only some of the oxygen atoms of the 18-crown-6 ring are also known, for example, $[\text{Li}(\text{18-crown-6})]\text{ClO}_4 \cdot 2\text{H}_2\text{O}$ ⁵² and $[\{\text{Li}(\text{NC}_5\text{H}_4\text{S-2})\}_2\text{-}(\text{18-crown-6})]$.⁵³

The structural changes in 18-crown-6 are smaller upon coordination to metal atoms than in D₆ (see Table 3). All O–C bonds are slightly lengthened in the complexes compared to free 18-crown-6. The lengthening in the silver(I) complexes correlates with the strength of the oxygen coordination to silver(I), with the largest difference observed for the oxygen atoms that are axially coordinated to silver(I) in the dinuclear $[\text{Ag}(\text{18-crown-6})]_2^{2+}$ complex. The calculated and experimental Li–O contacts in $[\text{Li}(\text{18-crown-6})]^+$ are shorter than the

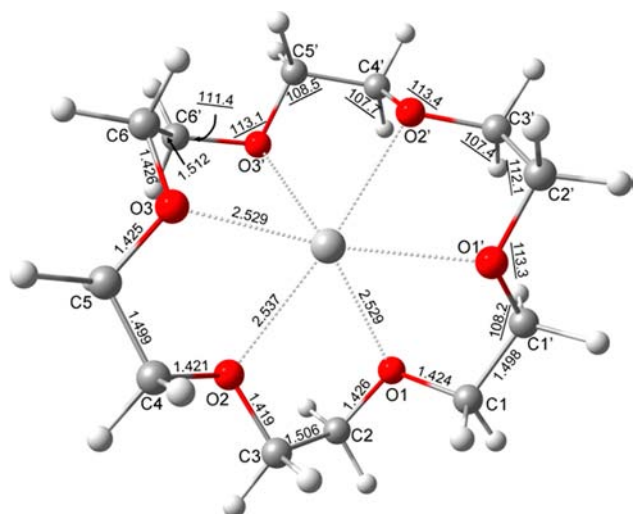


Figure 5. Optimized structure and selected structure parameters (bond lengths in Å, bond angles in deg) of $[\text{Ag}(18\text{-crown-6})]^+$ (C_2 symmetric).

Ag–O contacts in the mononuclear $[\text{Ag}(18\text{-crown-6})]^+$ complex similarly to the trend observed for the D_6 complexes. Contacts to metal atoms from the coordinating oxygen atoms O_c of 18-crown-6 are longer than the contacts from the coordinating oxygen atoms of D_6 in both the lithium and the silver(I) complexes with the exception of Ag– O_{ax} contact in $[\text{Ag}(18\text{-crown-6})]_2^{2+}$.

3.5. Gas Phase Binding Energies in Metal Complexes.

Theoretical gas phase lithium and silver(I) binding energies of 18-crown-6 and D_n ($n = 5-8$) have been calculated at the M06-L/6-311++G(2d,p) level to compare the relative binding strengths of the 18-crown-6 and D_6 metal complexes and to examine the stability trend of the metal complexes within the D_n series. The calculated gas phase binding energies are presented in Table 4. To get an estimate of the reliability of the calculated binding energies M06-L/6-311++G(2d,p) calculated proton affinity of 18-crown-6 ($-929.1 \text{ kJ mol}^{-1}$; For the structure of the protonated 18-crown-6 see the Supporting Information, Figure S4.2) was compared with a recently established experimental value from competitive threshold collision-induced dissociation measurements ($-935.3 \pm 11.4 \text{ kJ mol}^{-1}$),⁵⁴ and found to agree well with the experiment.

18-Crown-6 is calculated to bind more strongly to metal cations than D_6 similar to the trend reported for the relative metal binding strengths of simple ethers and siloxanes in previous studies.²¹ The binding energy difference for the 18-crown-6 and D_6 complexes calculated by DFT is somewhat smaller than the 100 kJ mol^{-1} reported for the Li^+ complexes at the HF/3-21G* level in our previous study.⁸ Part of the energy difference between the 18-crown-6 and D_6 complexes can be associated with the larger structural changes that D_6 goes through to accommodate the metal ions (cf energy differences between the complexed and free geometries of 18-crown-6 and D_6 in Table 7). However, the structural changes do not account for all of the binding energy difference between these complexes.

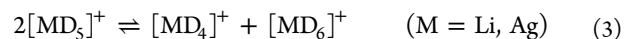
Lithium, being a harder Lewis acid than silver(I),⁵⁵ is calculated to bind more strongly to both 18-crown-6 and D_6 at the M06-L/6-311++G(2d,p) level of theory (as well as at the RI-MP2/def2-TZVPP level, see the Supporting Information, Table S4.1 for details). The stronger calculated binding of lithium to D_6 is in line with the relative coordination strengths in

Table 4. Gas Phase [M06-L/6-311++G(2d,p)] Lithium and Silver(I) Binding Energies (ΔE_{gas}), Enthalpies (ΔH_{gas}), and Free Binding Energies (ΔG_{gas}) (kJ mol^{-1}) of 18-Crown-6 and D_n ($n = 5-8$) and Relative Stabilities of Lithium and Silver(I) D_n Complexes^a

reaction	ΔE_{gas}	ΔH_{gas}	$\Delta G_{\text{gas}}(298 \text{ K})$
$\text{Li}^+ + 18\text{-crown-6} \rightleftharpoons [\text{Li}(18\text{-crown-6})]^+$	-416.0	-422.5	-372.7
$\text{Li}^+ + D_4 \rightleftharpoons [\text{Li}D_4]^+$	-241.4	-245.2	-205.0
$\text{Li}^+ + D_5 \rightleftharpoons [\text{Li}D_5]^+$	-286.8	-291.2	-252.0
$\text{Li}^+ + D_6 \rightleftharpoons [\text{Li}D_6]^+$	-332.3	-337.3	-294.9
$\text{Li}^+ + D_7 \rightleftharpoons [\text{Li}D_7]^+$	-373.5	-377.9	-333.5
$\text{Li}^+ + D_8 \rightleftharpoons [\text{Li}D_8]^+$	-331.9	-336.9	-296.5
$\text{Ag}^+ + 18\text{-crown-6} \rightleftharpoons [\text{Ag}(18\text{-crown-6})]^+$	-407.2	-411.1	-362.0
$\text{Ag}^+ + D_4 \rightleftharpoons [\text{Ag}D_4]^+$	-240.5	-241.4	-201.5
$\text{Ag}^+ + D_5 \rightleftharpoons [\text{Ag}D_5]^+$	-278.5	-279.4	-241.4
$\text{Ag}^+ + D_6 \rightleftharpoons [\text{Ag}D_6]^+$	-317.7	-320.1	-273.6
$\text{Ag}^+ + D_7 \rightleftharpoons [\text{Ag}D_7]^+$	-375.8	-376.7	-338.0
$\text{Ag}^+ + D_8 \rightleftharpoons [\text{Ag}D_8]^+$	-357.0	-357.8	-317.2
$2 D_5 \rightleftharpoons D_4 + D_6$	+3.8	+5.1	-1.1
$2 D_6 \rightleftharpoons D_5 + D_7$	+23.9	+22.0	+26.7
$2 D_7 \rightleftharpoons D_6 + D_8$	-40.7	-42.9	-27.3
$2 [\text{Li}D_5]^+ \rightleftharpoons [\text{Li}D_4]^+ + [\text{Li}D_6]^+$	+3.6	+5.0	+3.1
$2 [\text{Li}D_6]^+ \rightleftharpoons [\text{Li}D_5]^+ + [\text{Li}D_7]^+$	+28.2	+27.4	+30.9
$2 [\text{Li}D_7]^+ \rightleftharpoons [\text{Li}D_6]^+ + [\text{Li}D_8]^+$	+42.2	+38.9	+48.4
$2 [\text{Ag}D_5]^+ \rightleftharpoons [\text{Ag}D_4]^+ + [\text{Ag}D_6]^+$	+2.7	+2.4	+6.5
$2 [\text{Ag}D_6]^+ \rightleftharpoons [\text{Ag}D_5]^+ + [\text{Ag}D_7]^+$	+4.8	+6.0	-5.4
$2 [\text{Ag}D_7]^+ \rightleftharpoons [\text{Ag}D_6]^+ + [\text{Ag}D_8]^+$	+36.4	+32.8	+57.9

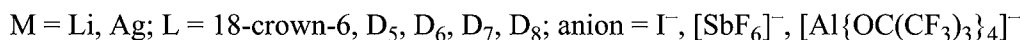
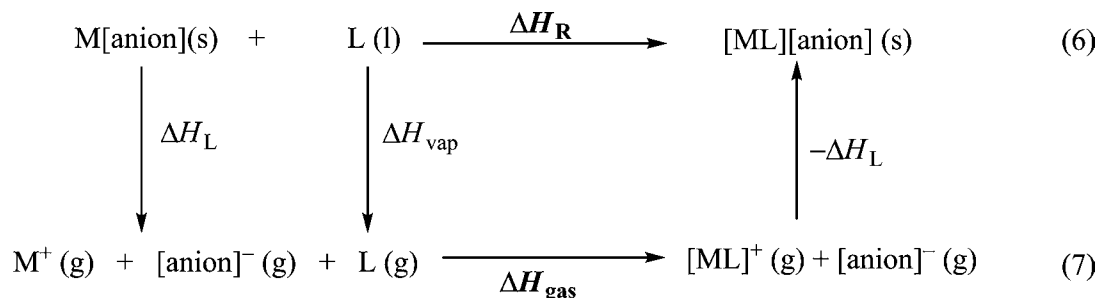
^aFor the calculated structures see the Supporting Information, Figure S4.3.

solution as suggested by the $^{29}\text{Si}\{^1\text{H}\}$ NMR. It is worth noting that this binding strength trend is opposite to what was found for the relative stabilities of the Li^+ and Ag^+ complexes of an acyclic siloxane $\text{O}(\text{SiH}_2\text{CH}_3)_2$ in our previous study.²¹ Within the D_n ($n = 5-8$) series the binding strength to lithium and silver(I) increases as the ring size increases up until D_7 that forms the most stable of the calculated D_n complexes. The smaller D_n rings are calculated to bind more strongly to lithium while the larger D_7 and D_8 rings tend to favor silver(I) in line with the relative sizes of the lithium and silver(I) cations. To further elucidate the relative stabilities of the D_n metal complexes the energetics of disproportionation reactions in eqs 3-5 have been considered.



The calculated reaction energies (See Table 4) suggest that for $[\text{Li}D_6]^+$ a disproportionation to $[\text{Li}D_5]^+$ and $[\text{Li}D_7]^+$ (eq 4) is unfavorable while for $[\text{Ag}D_6]^+$ the corresponding disproportionation is marginally favorable ($\Delta G_{\text{gas}} = -5.4 \text{ kJ mol}^{-1}$). For $[\text{MD}_5]^+$ and $[\text{MD}_7]^+$ ($\text{M} = \text{Li}, \text{Ag}$) the disproportionation reactions (eqs 3 and 5 respectively) are calculated to be unfavorable. A comparison with the disproportionation reactions of neutral D_n ($n = 5-7$) (see Table 4) indicates that the complexation of D_6 with Ag^+ destabilizes D_6 significantly compared to other rings (the disproportionation of neutral D_6 is disfavored by $+26.7 \text{ kJ mol}^{-1}$) while the metal complexation stabilizes D_5 and especially D_7 . The high relative stability of

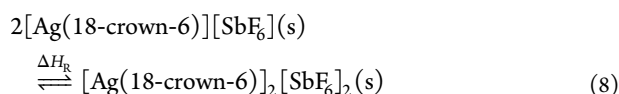
Scheme 1. Born–Fajans–Haber Cycle for the Formation of [ML][anion] Complexes in the Solid State



[MD₇]⁺ complexes is in contrast with the stability order of the neutral D_n rings that has been reported to favor the smaller rings.⁵⁶

The calculated metal cation binding and reaction energies for the D_n complexes give further evidence for the suggested stability order of the metal D_n complexes and justification for finding [AgD₇]⁺ as the major component and the isolated species in the AgSbF₆ + D_n reaction mixture in a previous study.¹⁰ The reaction energies also suggest that the equilibrium between the D_n rings can be moved toward the larger rings by templating the rings with suitable (metal) cations.

3.6. Solid State Binding Enthalpies in the Metal Complexes. The stabilities of cationic complexes in the solid state depend on the sizes of the complexes and anions that form the salts. With the aim of evaluating the effect counterions have on the stabilities of 18-crown-6 and D_n (n = 5–8) metal complexes in the solid state, the stabilities of different salts of the mononuclear complexes have been predicted using a Born–Fajans–Haber cycle shown in Scheme 1. The lattice enthalpies (ΔH_L) involved in the Born–Fajans–Haber cycle have been estimated by a volume based thermodynamics (VBT) approach.⁵⁷ To take into account the fact that silver(I) forms a dinuclear complex with 18-crown-6 and a 2:1 salt in **3**, the stability of **3** compared to the corresponding mononuclear complex in the solid has been estimated from eq 8.



The calculated solid state enthalpies (Table 5) establish that the 18-crown-6 metal complex salts of Li⁺ and Ag⁺ are stable with the anions of all considered sizes in good agreement with the characterization of structures like [Li(18-crown-6)]ClO₄·2H₂O⁵² and **3**. In the gas phase formation of the dinuclear [Ag(18-crown-6)]₂²⁺ complex from the mononuclear [Ag(18-crown-6)]⁺ complex is calculated to be endothermic by +103.5 kJ mol⁻¹, but in the solid state the high lattice energy from a 2:1 salt formed by [Ag(18-crown-6)]₂²⁺ drives the reaction 8 to the right giving a reaction enthalpy ΔH_R of –265 kJ mol⁻¹ (Details have been given in the Supporting Information, Section S5). The solid state reaction enthalpy is so exothermic that increasing the size of the anion further is most likely not going to be enough to stabilize the mononuclear [Ag(18-crown-6)]⁺ complex over the dinuclear [Ag(18-crown-6)]₂²⁺ unless there is a significant stabilizing coordination from the anion or solvent molecules (e.g., ΔH_R (eq 8) for a [Al{OC(CF₃)₃}₄]⁻ salt is –212 kJ mol⁻¹).

Table 5. Solid State Reaction Enthalpies ΔH_R for Formation (Scheme 1) of Lithium and Silver(I) 18-Crown-6 and D_n (n = 5–8) Complex Salts with Anions of Different Sizes

	I ⁻	[SbF ₆] ⁻	[Al{OC(CF ₃) ₃ } ₄] ⁻
[Li(18-crown-6)][anion]	-49	-114	-267
[LiD ₄][anion]	+59	-8	-168
[LiD ₅][anion]	+35	-32	-204
[LiD ₆][anion]	+11	-58	-237
[LiD ₇][anion]	-11	-81	-267
[LiD ₈][anion]	+44	-26	-217
[Ag(18-crown-6)][anion]	-48	-108	-256
[AgD ₄][anion]	+51	-10	-165
[AgD ₅][anion]	+36	-27	-192
[AgD ₆][anion]	+17	-47	-220
[AgD ₇][anion]	-22	-86	-266
[AgD ₈][anion]	+11	-54	-238

The stability of the dinuclear [Ag(18-crown-6)]₂²⁺ complex in the solid state is reminiscent of E₄²⁺[AsF₆]₂⁻ (S, Se, Te) and I₄²⁺[AsF₆]₂⁻ where the dicationic dimers are stabilized in the solid state by a gain in the lattice enthalpies.⁵⁸

According to the calculated solid state reaction enthalpies the D₆ metal complex salts of Li⁺ and Ag⁺ (see Table 5) with small anions are unlikely to be stable, but the [SbF₆]⁻ anion should be large enough to stabilize the complexes. The experimental attempts to make [AgD₆][SbF₆](s) have not been successful because the reactions led to D_n ring transformations and the isolation of the most stable D_n silver(I) complex salt [AgD₇][SbF₆] (see Table 5).¹⁰ The metal complexes of smaller D₄ and D₅ are calculated to be marginally stable with anions the size of [SbF₆]⁻. In conclusion the calculations suggest that the lithium and silver(I) complexes of the smaller D_n rings (n = 4, 5, 6) could be stabilized with weakly coordinating anions larger than [SbF₆]⁻ provided that ring transformation reactions can be inhibited.

The solid state reaction enthalpies retain the higher gas phase acidity of Li⁺ toward the smaller D_n (n = 4, 5, 6) compared to Ag⁺. The higher calculated stability of [LiD₆]⁺ is in contrast with the bond valence results from [LiD₆][Al{OC(CF₃)₃}₄] (sum of Li⁺–O contacts 0.810 v.u.)⁸ and **1** (sum of Ag⁺–O contacts 0.954 v.u.). The energy differences between the solid state stabilities of [LiD₆]⁺ and [AgD₆]⁺ salts are well within the accuracy of the VBT approach,⁵⁹ but the difference can also be related to structural differences between the calculated and experimental complex structures. Unlike the bond valences determined from the crystal structures the sums of the bond valences of the metal oxygen contacts for optimized structures

agree with the calculated energies that suggest lithium to be more strongly coordinated to D_6 than silver(I) (c.f. $[\text{LiD}_6]^+$ 0.953 v.u. vs $[\text{AgD}_6]^+$ 0.914 v.u.). The lower coordination strength of Li^+ to D_6 indicated by the bond valences of the $[\text{LiD}_6][\text{Al}\{\text{OC}(\text{CF}_3)_3\}_4]$ crystal structure is therefore most likely because of the closer proximity of the anions and cations in $[\text{LiD}_6][\text{Al}\{\text{OC}(\text{CF}_3)_3\}_4]$ compared to **1** (c.f. $\text{Li}^+\cdots\text{F}$ 2.641(16) Å in $[\text{LiD}_6][\text{Al}\{\text{OC}(\text{CF}_3)_3\}_4]$ and $\text{Ag}^+\cdots\text{F}$ 2.980(3) Å in **1**, see Figure 1a) that weakens the Li^+-O contacts in the crystal structure compared to the calculated structure (see Table 3).

3.7. QTAIM Analysis of the Bonding in D_6 and 18-Crown-6 Metal Complexes. Our theoretical studies on Li^+ and Ag^+ complexes of 1,3-dimethyldisiloxane and diethyl ether have shown that the electron donation strengths of $\text{O}(\text{SiH}_2\text{Me})_2$ and OEt_2 to metal ions are similar and the electrostatic interactions between the metal ions and ligands in the complexes are comparable.²¹ The calculations also suggested that the stability differences between the siloxane and ether complexes arise from the structural changes in the ligands and the polarization of the $\text{O}-\text{X}$ bonds ($\text{X} = \text{Si}, \text{C}$) in the presence of metal ions that raise the energy of $\text{O}(\text{SiH}_2\text{Me})_2$ more upon complexation than the energy of OEt_2 . To assess if the stability differences of the D_6 and 18-crown-6 metal complexes of Li^+ and Ag^+ are due to the same reasons, atomic charges and delocalization indices (DIs) of selected bonds in the D_6 and 18-crown-6 metal complex structures have been determined by the QTAIM method⁶⁰ and presented in Table 6. For comparison

Table 6. Comparison of Average QTAIM Charges and Delocalization Indices (DI) of Calculated D_6 and 18-Crown-6 Complexes of Lithium and Silver(I)^{a,b}

		charge		DI
D_6 (C_i)	O	-1.64	O-Si	0.39
	Si	+3.04		
$[\text{LiD}_6]^+$ (C_2)	Li	+0.92	Li- O_c	0.06
	O_c	-1.66	Li- O_{wc}	0.00
	O_{wc}	-1.63	O_c -Si	0.36
	Si	+3.03	O_{wc} -Si	0.39
$[\text{AgD}_6]^+$ (C_3)	Ag	+0.74	Ag- O_c	0.32
	O_c	-1.61	Ag- O_{wc}	0.10
	O_{wc}	-1.63	O_c -Si	0.36
	Si	+3.03	O_{wc} -Si	0.38
(18-crown-6) (C_i)	O	-1.06	O-C	0.87
	C	+0.53		
$[\text{Li}(18\text{-crown-6})]^+$ (D_2)	Li	+0.92	Li-O	0.04
	O	-1.08	O-C	0.86
	C	+0.50		
$[\text{Ag}(18\text{-crown-6})]^+$ (calc. C_2)	Ag	+0.73	Ag-O	0.21
	O	-1.05	O-C	0.86
	C	+0.50		
$[\text{Ag}(18\text{-crown-6})]_2^{2+}$ (calc. C_i)	Ag	+0.75	Ag- O_c	0.19
	O_c	-1.06	Ag- O_{wc}	0.11
	O_{wc}	-1.05	Ag- O_{ax}	0.22
	$O_{wc/ax}$	-1.04	O_c -C	0.85
	C	+0.50	$O_{wc/ax}$ -C	0.85

^a c = coordinated, wc = weakly coordinated, ax = axially coordinated.

^bM06-L/6-311++G(2d,p) wave function.

the natural bond orbital (NBO) analysis results have been presented in the Supporting Information, Section 6. The NBO results suggested a different but not as consistent bonding

picture as the QTAIM description given here and have not been considered further.

Atomic charges on silicon atoms in D_6 are calculated to be much higher than atomic charges on carbon atoms in 18-crown-6, and oxygen atomic charges in D_6 are more negative than those in 18-crown-6. Added to the atomic charges the lower DI values of Si-O bonds compared to C-O bonds indicate the higher ionic nature of the Si-O bonds. The differences between the Si-O bonds in D_6 and the C-O bonds in 18-crown-6 reflect those found previously for the bonds in $\text{O}(\text{SiH}_2\text{Me})_2$ and OEt_2 .²¹

In the calculated complex structures all of the oxygen atoms of 18-crown-6 and D_6 coordinate to the lithium and silver(I) atoms except for $[\text{LiD}_6]^+$, where only four oxygen atoms are connected to the lithium atom by a bond path. In the lithium complexes the oxygen atomic charges on the coordinating oxygen atoms in D_6 and 18-crown-6 become more negative compared to the free molecules (see Table 6). This indicates a polarization of the molecules by the metal ion similar to what was found in the lithium complexes of OEt_2 and $\text{O}(\text{SiH}_2\text{Me})_2$.²¹ The polarization of D_6 and 18-crown-6 by metal ions is not as pronounced as the calculated polarization of OEt_2 and $\text{O}(\text{SiH}_2\text{Me})_2$ was due to the weaker individual oxygen metal interactions that result from the longer contacts (c.f. calculated Li-O 1.809 Å in $[\text{LiOEt}_2]^+$ ²¹ and 2.120 Å in $[\text{Li}(18\text{-crown-6})]^+$). In the silver(I) complexes the atomic charges of the coordinating oxygen atoms are slightly less negative than in free D_6 and 18-crown-6. The less negative atomic charges on the oxygen atoms are related to the low atomic charges on the silver(I) atoms and the relatively high Ag-O DI values (e.g., Ag- O_c 0.32 in $[\text{AgD}_6]^+$), that indicate a significant electron transfer from both D_6 and 18-crown-6 to silver(I) in the complex structures.

The atomic charges and the DI values suggest that donation from 18-crown-6 and D_6 to metal ions is of similar strength. This implies that the stability difference between the 18-crown-6 and D_6 metal complexes is either caused by the differences in the electrostatic interactions between the metal ions and the ligands and/or the structural and bonding changes in 18-crown-6 and D_6 upon complexation. By calculating the energy differences ΔE_{geom} between the free and complex geometries of 18-crown-6 and D_6 molecules (see Table 7), it can be shown that the

Table 7. Energy Changes ΔE_{geom} (kJ mol^{-1}) for 18-Crown-6 and D_6 Going from Free Ligand Geometries to Complex Geometries in Lithium and Silver(I) Complexes and IQA Classical, E_{cl} , and Exchange-Correlation, E_{XC} , Energy Contributions to Metal Ligand Binding in the Complexes [HF/6-311++G(2d,p) Wavefunction]

	ΔE_{geom}	E_{cl}	E_{XC}
$[\text{Li}(18\text{-crown-6})]^+$	+68.4	-596	-114
$[\text{LiD}_6]^+$	+74.8	-512	-127
$[\text{Ag}(18\text{-crown-6})]^+$	+43.8	-289	-529
$[\text{AgD}_6]^+$	+65.3	-251	-513

structural changes account for a part of the stability difference of the complexes but are not the major contributor to the different stabilities.

Interacting quantum atoms (IQA) energy decomposition analysis is a convenient method for estimating the covalent and electrostatic contributions to bonding.⁶¹ The IQA analysis allows a division of the binding energies to deformation energies E_{def} of the bonded groups,⁶² exchange-correlation E_{XC} (covalent)

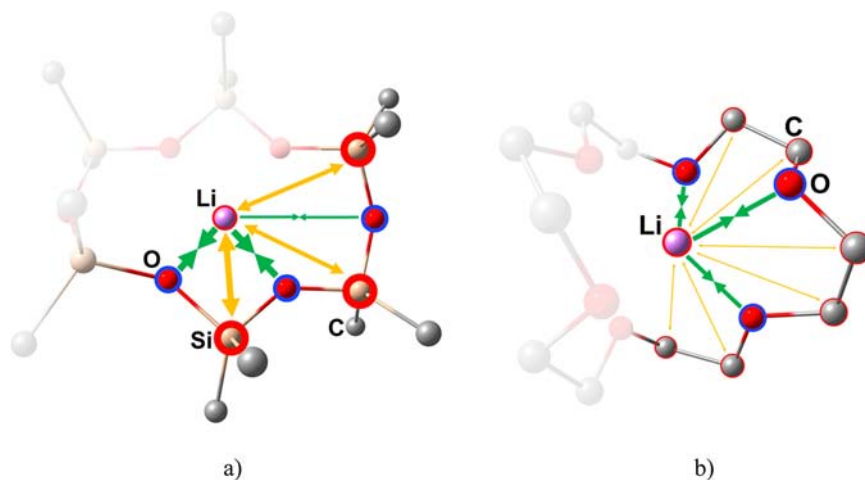


Figure 6. Qualitative illustration of the attractive and repulsive electrostatic interactions between lithium and ligand atoms in (a) $[\text{LiD}_6]^+$ and (b) $[\text{Li}(18\text{-crown-6})]^+$ complexes. Hydrogen atoms and parts of the D_6 and 18-crown-6 rings have been removed for clarity.

contributions, and classical E_{cl} (electrostatic) contributions to the binding energies according to eq 9.

$$E_{\text{bind}} = \sum_A E_{\text{def}}^A + \sum_{A>B} (E_{\text{XC}}^{AB} + E_{\text{cl}}^{AB}) \quad (9)$$

where A and B are atoms or group of atoms.

An IQA analysis was used in our previous study for the OEt_2 and $\text{O}(\text{SiH}_2\text{Me})_2$ complexes of Li^+ and Ag^+ to show that the electrostatic interactions between the metal ions and both ligands were similar and the stability differences of the complexes were due to changes in the bonds of the ligands.^{21,63} Unfortunately full IQA energy decomposition analyses for the 18-crown-6 and D_6 complexes of lithium and silver(I) are beyond the computational resources available to us because of the high computational effort related to the calculation of the E_{def} of the ligands.³¹ However, estimates of the exchange-correlation E_{XC} and the classical E_{cl} contributions to the metal binding can be made from integrations on the Li^+ and Ag^+ ions in the complexes. The estimated exchange-correlation E_{XC} and classical E_{cl} metal binding energies are presented in Table 7. The E_{XC} in the silver(I) complexes compared to the lithium complexes are much higher in good agreement with the more extensive electron donation suggested by the atomic charges and the DI values (see Table 6). The similarity of the E_{XC} in the 18-crown-6 and D_6 complexes gives further support for the similar donation strengths of 18-crown-6 and D_6 suggested by the atomic charges and the DI values. The electrostatic metal binding energies E_{cl} are calculated more attractive for the 18-crown-6 complexes compared to the D_6 complexes (e.g., the difference in Li^+ complexes -84 kJ mol^{-1}) even though the oxygen atoms are calculated to be more negative in D_6 . The weaker electrostatic binding of the metal ions by D_6 can be related to the repulsion between the positively charged silicon atoms and the metal ions (See Figure 6) similar to what was found previously for the OEt_2 and $\text{O}(\text{SiH}_2\text{Me})_2$ metal complexes.²¹ The difference in the electrostatic interactions in the 18-crown-6 and D_6 metal complexes is in contrast to the OEt_2 and $\text{O}(\text{SiH}_2\text{Me})_2$ metal complexes where the electrostatic interactions between the metal ions and the ligands were similar. Presumably this difference is caused by the constraints the ring structures impose on the charge distributions in the 18-crown-6 and D_6 metal complexes.

In the OEt_2 and $\text{O}(\text{SiH}_2\text{Me})_2$ metal complexes (of Li^+ and Ag^+) the main contributions to the stability differences were from the deformation energies of the ligands.²¹ The differences in the deformation energies were attributed to the differences in the polarization of O-X ($\text{X} = \text{C}, \text{Si}$) bonds by metal ions. In the 18-crown-6 and D_6 complexes the polarization of the O-X bonds by Li^+ and Ag^+ ions are calculated to be less than those in the OEt_2 and $\text{O}(\text{SiH}_2\text{Me})_2$ metal complexes, respectively, and therefore the contribution of polarization effects to the stability differences of the complexes can be expected to be smaller. Although the calculation of deformation energies for the 18-crown-6 and D_6 complexes was not feasible their contribution to the stability differences of the complexes can be estimated by comparing the sums of the other terms (E_{cl} and E_{XC}) in eq 9 to the differences in the binding energies. The differences in the sums of E_{cl} and E_{XC} in the 18-crown-6 and D_6 complexes of Li^+ and Ag^+ are 71 and 54 kJ mol^{-1} , respectively (see Table 7). The corresponding differences in the metal binding energies of Li^+ and Ag^+ complexes are 84 and 90 kJ mol^{-1} , and a comparison of these shows that the differences in the deformation energies account for 13 and 36 kJ mol^{-1} of the stability differences in the Li^+ and Ag^+ complexes, respectively. Furthermore, the deformation energies can be divided into energy changes due to structural changes going from free to bound geometries and changes in the bonding and polarization of the bound groups. The magnitude of how the changes in the bonding and polarization of 18-crown-6 and D_6 upon complex formation affect the relative stabilities of the 18-crown-6 and D_6 complexes of Li^+ and Ag^+ can be estimated by subtracting the energy changes due to the structural changes in ligands ΔE_{geom} (see Table 7) and assuming the metal deformation energies are similar in both the 18-crown-6 and D_6 complexes. The subtraction of ΔE_{geom} from the deformation energy difference suggests that changes in the polarization and bonding of 18-crown-6 and D_6 account for 7 and 15 kJ mol^{-1} of the stability differences in the Li^+ and Ag^+ complexes, respectively. In agreement with the small changes in the atomic charges and the DIs the changes in the bonding and polarization of 18-crown-6 and D_6 account only for a small part of the stability difference of the complexes. Therefore the main contributions to the stability differences between the 18-crown-6 and D_6 metal complexes are due to the electrostatic interactions that are more attractive between 18-crown-6 and the metal ions. These results emphasize the importance the

electrostatic interactions can have in explaining the differences in the bonding of other compounds of the second period and heavier main group elements (e.g., pyramidal $\text{N}(\text{CH}_3)_3$ vs planar $\text{N}(\text{SiH}_3)_3$).^{19a,64}

4. CONCLUSIONS

The syntheses and characterization of $[\text{AgD}_6][\text{Al}]$ ($[\text{Al}] = \text{Al}(\text{OR}_F)_4, \text{AlF}(\text{OR}_F)_3$) salts presented in this paper provide the first examples of a preparation of transition metal ion host-guest complexes of cyclic dimethylsiloxanes directly from the components. We have shown that metal complexes of cyclic dimethylsiloxanes can be prepared via two routes in $\text{SO}_2(\text{l})$: Ring transformations with soluble $[\text{MF}_6]^-$ salts leading to the thermodynamically most stable complexes, and reactions with $[\text{Al}]^-$ salts giving the metal complex of a starting D_n . A requisite for the reactions is the use of very weakly coordinating solvents, for example, addition of CH_3CN to reaction mixture was shown to replace the D_n in the complexes.¹⁰

DFT calculations have been used to study the structures and stabilities of $[\text{MD}_n]^+$ ($\text{M} = \text{Ag}, \text{Li}, n = 4-8$) complexes. In contrast to a previous electron diffraction report that has suggested D_6 to have a D_{3d} symmetric structure,⁴⁴ a puckered C_i symmetric structure was predicted as the minimum structure by calculations. Li^+ was shown to be a stronger acid than Ag^+ toward D_6 by calculations in the gas phase and by the $^{29}\text{Si}[\text{H}]$ NMR in solution. A comparison of the gas and solid state stabilities of the $[\text{MD}_n]^+$ ($\text{M} = \text{Ag}, \text{Li}, n = 4-8$) complexes revealed that the larger D_n could be stabilized with respect to the smaller rings by templating the rings with suitable (metal) ions. This work together with previous reports^{8,10,21} implies that numerous salts of metal cyclodimethylsiloxane complexes and even acyclic siloxane metal complexes can be prepared by the reactions of siloxanes with metal salts of weakly coordinating anions in very weakly coordinating solvents, for example, SO_2 .

Dinuclear $[\text{Ag}(\text{18-crown-6})]_2[\text{SbF}_6]_2$ is a rare example of a solvent free silver(I) 18-crown-6 complex. The formation of the dinuclear $[\text{Ag}(\text{18-crown-6})]_2[\text{SbF}_6]_2$ complex instead of the alternative mononuclear complex in the solid state was shown to be driven by the gain in lattice enthalpy on formation of a 2:1 salt compared to a 1:1 salt. A comparison of bonding in the 18-crown-6 and D_6 metal complexes confirms the expected result that siloxane is a weaker base toward Ag^+ and Li^+ ions. QTAIM bond analyses described the bonding to lithium from D_6 and 18-crown-6 to be predominately electrostatic while the bonding to silver(I) showed also a charge transfer from oxygen atoms to the silver(I) ions. The QTAIM results indicated that the charge transfer from both D_6 and 18-crown-6 to metal ions (Li^+, Ag^+) is similar and suggested that the stability differences between the D_6 and 18-crown-6 complexes arise from the differences in the electrostatic interactions. The electrostatic interactions were calculated to be more attractive between 18-crown-6 and the metal ions despite the more negative oxygen atomic charges calculated for the D_6 oxygen atoms. The weaker electrostatic attraction between D_6 and the metal ions is attributed to the repulsion between the positively charged silicon atoms and the metal ions similarly to what was found earlier for smaller disiloxane metal complexes.²¹

■ ASSOCIATED CONTENT

Supporting Information

FT-IR spectra of 1–3, comparison of the chemical shifts in related compounds, crystal packing figures for 1–3, structural parameter comparisons of the cations and anions in 1–3, and in related compounds, M06-L optimized structures of the D_n ,

$[\text{MD}_n]^+$ complexes ($\text{M} = \text{Li}, \text{Ag}, n = 4-8$), and $[\text{H}(\text{18-crown-6})]^+$, details of the VBT calculations, NBO analysis results, and IQA analysis results of $[\text{LiO}(\text{SiH}_2\text{CH}_3)_2]^+$ as a function of Li–O distance. CCDC reference numbers 924382, 902385, 902386. This material is available free of charge via the Internet at <http://pubs.acs.org>.

■ AUTHOR INFORMATION

Corresponding Author

*Fax: (+1) 506-453-4981 (J.P.). E-mail: passmore@unb.ca (J.P.), mikko.rautainen@oulu.fi (J.M.R.).

Notes

The authors declare no competing financial interest.

■ ACKNOWLEDGMENTS

We thank the Natural Sciences and Engineering Research Council (NSERC) of Canada (J.P.) and Academy of Finland (J.M.R) for funding. ACEnet, the regional high performance computing consortium for universities in Atlantic Canada and CSC—IT Center for Science Ltd. in Finland are acknowledged for providing computational resources.

■ REFERENCES

- (1) Pedersen, C. J. *J. Am. Chem. Soc.* **1967**, *89*, 7017.
- (2) (a) Alexeev, Yu. E.; Kharisov, B. I.; Hernández García, T. C.; Garnovskii, A. D. *Coord. Chem. Rev.* **2010**, *254*, 794. (b) Gokel, G. W.; Leevy, W. M.; Weber, M. E. *Chem. Rev.* **2004**, *104*, 2723. (c) Goldberg, I. In *Inclusion Compounds*; Atwood, J. L., Davies, J. E. D., MacNicol, D. D., Eds.; Academic Press: London, U.K., 1984; Vol. 2, pp 261–335.
- (3) Pedersen, C. J. In *Nobel lectures, Chemistry*; Frängsmyr, T., Malmström, B. G., Eds.; World Scientific Publishing: Singapore, 1992; pp 496–511.
- (4) Ritch, J. S.; Chivers, T. *Angew. Chem., Int. Ed.* **2007**, *46*, 4610.
- (5) (a) Genualdi, S.; Harner, T.; Cheng, Y.; MacLeod, M.; Hansen, K. M.; van Egmond, R.; Shoeib, M.; Lee, S. C. *Environ. Sci. Technol.* **2011**, *45*, 3349. (b) Wang, R.; Moody, R. P.; Koniecki, D.; Zhu, J. *Environ. Int.* **2009**, *35*, 900. (c) Horii, Y.; Kannan, K. *Arch. Environ. Contam. Toxicol.* **2008**, *55*, 701.
- (6) Churchill, M. R.; Lake, C. H.; Chao, S. H.; Beachley, J. O. T. *J. Chem. Soc., Chem. Commun.* **1993**, 1577.
- (7) Eaborn, C.; Hitchcock, P. B.; Izod, K.; Smith, J. D. *Angew. Chem., Int. Ed. Engl.* **1995**, *34*, 2679; *Angew. Chem.* **1995**, *23*, 2936.
- (8) Decken, A.; Passmore, J.; Wang, X. *Angew. Chem., Int. Ed.* **2006**, *45*, 2773.
- (9) Ernst, R. D.; Glöckner, A.; Arif, A. M. Z. *Kristallogr.* **2007**, *222*, 333.
- (10) Decken, A.; LeBlanc, F. A.; Passmore, J.; Wang, X. *Eur. J. Inorg. Chem.* **2006**, 4033.
- (11) Krossing, I.; Raabe, I. *Chem.—Eur. J.* **2004**, *10*, 5017.
- (12) Witek, G.; Siebenhofer, M.; Uhlig, F. *Chem. Ing. Tech.* **2009**, *81*, 1050.
- (13) Passmore, J.; Wang X., unpublished observations.
- (14) Bagatur'yants, A. A.; Freidzon, A. Ya.; Alfimov, M. V.; Baerends, E. J.; Howard, J. A. K.; Kuz'mina, L. G. *J. Mol. Struct.(Theochem)* **2002**, *588*, 55.
- (15) Steed, J. W.; Johnson, K.; Legido, C.; Junk, P. C. *Polyhedron* **2003**, *22*, 769.
- (16) Wang, Q.-M.; Mak, T. C. W. *Chem.—Eur. J.* **2003**, *9*, 44.
- (17) (a) West, R.; Whatley, L.; Lake, K. J. *Am. Chem. Soc.* **1961**, *83*, 761. (b) Shepherd, B. D. *J. Am. Chem. Soc.* **1991**, *113*, 5581, and references therein.
- (18) (a) Weinhold, F.; West, R. *Organometallics* **2011**, *30*, 5815. (b) Shambayati, S.; Blake, J. F.; Wierschke, S. G.; Jorgensen, W. L.; Schreiber, S. L. *J. Am. Chem. Soc.* **1990**, *112*, 697.

- (19) (a) Gillespie, R. J.; Robinson, E. A. *Chem. Soc. Rev.* **2005**, *34*, 396. (b) Gillespie, R. J.; Johnson, S. A. *Inorg. Chem.* **1997**, *36*, 3031. (c) Oberhammer, H.; Boggs, J. E. *J. Am. Chem. Soc.* **1980**, *102*, 7241.
- (20) (a) Grabowsky, S.; Beckmann, J.; Luger, P. *Aust. J. Chem.* **2012**, *65*, 785. (b) Grabowsky, S.; Hesse, M. F.; Paulmann, C.; Luger, P.; Beckmann, J. *Inorg. Chem.* **2009**, *48*, 4384.
- (21) Passmore, J.; Rautiainen, J. M. *Eur. J. Inorg. Chem.* **2012**, 6002.
- (22) Murchie, M. P.; Passmore, J.; Kapoor, R. *Inorg. Syntheses* **1997**, *31*, 102.
- (23) (a) Decken, A.; Knapp, C.; Nikiforov, G. B.; Rautiainen, J. M.; Passmore, J.; Wang, X.; Zheng, X. *Chem.—Eur. J.* **2009**, *15*, 6504–6517. (b) Krossing, I.; Gonsior, M.; Müller, L. U.S. Patent 20080033195, 2008.
- (24) *CrystalStructure 3.8: Crystal Structure Analysis Package*; Rigaku: The Woodlands, TX.
- (25) *SHELXTL*, 6.14; Bruker AXS, Inc.: Madison, WI, 2000–2006.
- (26) Brandenburg, K.; Brandt, M. *DIAMOND 3.2h*; Crystal Impact: Bonn, Germany.
- (27) Frisch, M. J.; Trucks, G. W.; Schlegel, H. B.; Scuseria, G. E.; Robb, M. A.; Cheeseman, J. R.; Scalmani, G.; Barone, V.; Mennucci, B.; Petersson, G. A.; Nakatsuji, H.; Caricato, M.; Li, X.; Hratchian, H. P.; Izmaylov, A. F.; Bloino, J.; Zheng, G.; Sonnenberg, J. L.; Hada, M.; Ehara, M.; Toyota, K.; Fukuda, R.; Hasegawa, J.; Ishida, M.; Nakajima, T.; Honda, Y.; Kitao, O.; Nakai, H.; Vreven, T.; Montgomery, Jr., J. A.; Peralta, J. E.; Ogliaro, F.; Bearpark, M.; Heyd, J. J.; Brothers, E.; Kudin, K. N.; Staroverov, V. N.; Kobayashi, R.; Normand, J.; Raghavachari, K.; Rendell, A.; Burant, J. C.; Iyengar, S. S.; Tomasi, J.; Cossi, M.; Rega, N.; Millam, N. J.; Klene, M.; Knox, J. E.; Cross, J. B.; Bakken, V.; Adamo, C.; Jaramillo, J.; Gomperts, R.; Stratmann, R. E.; Yazyev, O.; Austin, A. J.; Cammi, R.; Pomelli, C.; Ochterski, J. W.; Martin, R. L.; Morokuma, K.; Zakrzewski, V. G.; Voth, G. A.; Salvador, P.; Dannenberg, J. J.; Dapprich, S.; Daniels, A. D.; Farkas, Ö.; Foresman, J. B.; Ortiz, J. V.; Cioslowski, J.; Fox, D. J. *Gaussian 09*, Revision C.01; Gaussian, Inc.: Wallingford, CT, 2009.
- (28) (a) Zhao, Y.; Truhlar, D. G. *J. Chem. Phys.* **2006**, *125*, 194101. (b) Zhao, Y.; Truhlar, D. G. *Theor. Chem. Acc.* **2008**, *120*, 215.
- (29) (a) Krishnan, R.; Binkley, J. S.; Seeger, R.; Pople, J. A. *J. Chem. Phys.* **1980**, *72*, 650. (b) McLean, A. D.; Chandler, G. S. *J. Chem. Phys.* **1980**, *72*, 5639. (c) Clark, T.; Chandrasekhar, J.; Spitznagel, G. W.; Schleyer, P. v. R. *J. Comput. Chem.* **1983**, *4*, 294. (d) Frisch, M. J.; Pople, J. A.; Binkley, J. S. *J. Chem. Phys.* **1984**, *80*, 3265.
- (30) Peterson, K. A.; Puzzarini, C. *Theor. Chem. Acc.* **2005**, *114*, 283.
- (31) Keith, T. A. *AIMAll*, Version 12.06.03; 2012; aim.tkgristmill.com.
- (32) Zhurko, G. A. *ChemCraft*, 1.7; www.chemcraftprogr.com.
- (33) Vij, A.; Wilson, W. W.; Vij, V.; Tham, F. S.; Sheehy, J. A.; Christe, K. O. *J. Am. Chem. Soc.* **2001**, *123*, 6308.
- (34) Begun, G. M.; Rutenberg, A. C. *Inorg. Chem.* **1967**, *6*, 2212.
- (35) Nakamoto, K. *Infrared and Raman Spectra of Inorganic and Coordination compounds*, 4th ed.; Wiley-Interscience: Toronto, Canada, 1986.
- (36) (a) Takeuchi, H.; Arai, T.; Harada, I. *J. Mol. Struct.* **1986**, *146*, 197. (b) Sato, H.; Kasumoto, Y. *Chem. Lett.* **1978**, 635.
- (37) Kidd, R. G.; Matthews, R. W. *Inorg. Chem.* **1972**, *11*, 1156.
- (38) Decken, A.; Ilyin, E. G.; Jenkins, H. D. B.; Nikiforov, G. B.; Passmore, J. *Dalton Trans.* **2005**, 3039.
- (39) Gillespie, R. J.; Moss, K. C. *J. Chem. Soc. A* **1966**, 1170.
- (40) Wilson, M. J.; Pethrick, R. A.; Pugh, D.; Saiful Islam, M. *Faraday Trans.* **1997**, *93*, 2097.
- (41) The bond valences s (in valence units vu) are defined as $s = \exp[(R_0 - R)/B]$, where R is the observed distance, R_0 is the covalent bond length of the bond (bond order = 1; for Ag-F, $R_0 = 1.80 \text{ \AA}$; for Ag-O, $R_0 = 1.84 \text{ \AA}$; for Li-O, $R_0 = 1.466 \text{ \AA}$; for Li-N, $R_0 = 1.61 \text{ \AA}$), and B is an empirical parameter set to 0.37. (a) Brown, I. D. In *Structure and Bonding in Crystals*; Keefe, M. O. T., Navrotsky, A., Eds.; Academic Press: London, U.K., 1981; Vol. 2. (b) Brown, I. D. *The Chemical Bond in Inorganic Chemistry (The Bond Valence Model)*; Oxford University Press: Oxford, U.K., 2002.
- (42) Cameron, T. S.; Nikiforov, G. B.; Passmore, J.; Rautiainen, J. M. *Dalton Trans.* **2010**, *39*, 2587.
- (43) RI-MP2/def2-TZVPP energies have been determined as single point energies on M06-L/6-311++G(2d,p) optimized geometries. See Supporting Information, Section S4 for details.
- (44) Oberhammer, H.; Zeil, W.; Fogarasi, G. *J. Mol. Struct.* **1973**, *18*, 309.
- (45) Maverick, E.; Seiler, P.; Schweizer, W. B.; Dunitz, J. D. *Acta Crystallogr.* **1980**, *B36*, 615.
- (46) Hitchcock, P. B.; Hulkes, A. G.; Lappert, M. F.; Protchenko, A. V. *Inorg. Chim. Acta* **2006**, *359*, 2998.
- (47) Fogarasi, G.; Hacker, H.; Hoffmann, V.; Dobos, S. *Spectrochim. Acta* **1974**, *30A*, 629.
- (48) Alvik, T.; Dale, J. *Acta Chem. Scand.* **1971**, *25*, 2131.
- (49) Wagner, A. J.; Vos, A. *Acta Crystallogr.* **1968**, *B24*, 1423.
- (50) Spirk, S.; Belaj, F.; Nieger, M.; Köfeler, H.; Rechberger, G. N.; Pietschnig, R. *Chem.—Eur. J.* **2009**, *15*, 9521.
- (51) (a) Martínez-Haya, B.; Hurtado, P.; Hortal, A. R.; Hamad, S.; Steill, J. D.; Oomens, J. *J. Phys. Chem. A* **2010**, *114*, 7048. (b) Glendening, E. D.; Feller, D.; Thompson, M. A. *J. Am. Chem. Soc.* **1994**, *116*, 10657. (c) Bruna, P. J.; Greer, S.; Passmore, J.; Rautiainen, J. M. *Inorg. Chem.* **2011**, *50*, 1491.
- (52) Groth, P. *Acta Chem. Scand.* **1982**, *A36*, 109.
- (53) Chadwick, S.; Ruhlandt-Senge, K. *Chem.—Eur. J.* **1998**, *4*, 1768.
- (54) Chen, Y.; Rodgers, M. T. *Anal. Chem.* **2012**, *84*, 7570.
- (55) Pearson, R. G. *J. Am. Chem. Soc.* **1963**, *85*, 3533.
- (56) (a) Brown, J. F.; Slusarczuk, G. M. *J. Am. Chem. Soc.* **1965**, *87*, 931. (b) Carmichael, J. B.; Winger, R. J. *Polym. Sci.* **1965**, *A3*, 971.
- (57) Jenkins, H. D. B.; Roobottom, H. K.; Passmore, J.; Glasser, L. *Inorg. Chem.* **1999**, *38*, 3609.
- (58) (a) Cameron, T. S.; Dionne, I.; Jenkins, H. D. B.; Parsons, S.; Passmore, J.; Roobottom, H. K. *Inorg. Chem.* **2000**, *39*, 2042. (b) Brownridge, S.; Krossing, I.; Passmore, J.; Jenkins, H. D. B.; Roobottom, H. K. *Coord. Chem. Rev.* **2000**, *197*, 397.
- (59) Byrd, E. F. C.; Rice, B. M. *J. Phys. Chem. A* **2009**, *113*, 345.
- (60) Bader, R. W. F. *Atoms in molecules - A quantum theory*; Oxford University Press: Oxford, U.K., 1990.
- (61) (a) Blanco, M. A.; Pendás, A. M.; Francisco, E. J. *Chem. Theory Comput.* **2005**, *1*, 1096. (b) Pendás, A. M.; Blanco, M. A.; Francisco, E. J. *Comput. Chem.* **2007**, *28*, 161.
- (62) Deformation energies are sometimes called promotion energies and give an energetic penalty suffered by a group upon bond formation because of change in the optimum geometry of the group, interatomic charge transfer, and following charge reorganization (e.g., polarization).
- (63) Analysis of the IQA energy components of $[\text{LiO}(\text{SiH}_2\text{CH}_3)_2]^+$ structures at different Li–O distances showed that the increase in E_{def} due to bonding changes in $\text{O}(\text{SiH}_2\text{CH}_3)_2$ as the Li–O distance was shortened was compensated by the increase in E_{XC} and E_{el} all the way to the optimized geometry resulting in the most favorable binding of the lithium by $\text{O}(\text{SiH}_2\text{CH}_3)_2$ at that geometry. See the Supporting Information, Section S7 for details.
- (64) (a) Noodleman, N.; Paddock, N. L. *Inorg. Chem.* **1979**, *18*, 354. (b) Mo, Y.; Zhang, Y.; Gao, J. *J. Am. Chem. Soc.* **1999**, *121*, 5737.